1996ApJ...465..578S

THE ASTROPHYSICAL JOURNAL, 465:578–594, 1996 July 10
© 1996. The American Astronomical Society. All rights reserved. Printed in U.S.A.

TESTS OF LOCAL REDSHIFT-DISTANCE LAWS ON THE BASIS OF A COMPLETE OPTICAL SAMPLE

I. E. SEGAL[1] AND J. F. NICOLL[2]
Received 1994 September 7; accepted 1996 January 29

ABSTRACT

The linear and square (homogeneous quadratic) redshift-distance laws are tested statistically at redshifts $\lesssim 0.01$, on the basis of the whole-sky complete sample of elliptical type galaxies of Visvanathan and conservative subsamples. Objective estimates are made of the probabilities of deviations as large as the actual ones between the prediction and direct observation, by statistically efficient and equitable methods. Luminosity functions are also estimated and tested for consistency. Sample statistics corrected for the observational magnitude cutoff, on the basis of the estimated luminosty functions, are reported.

As in the case of the infrared and X-ray wave bands, the predictions of the linear law appear to be significantly deviant from the observations, by 7 σ at the reported completeness level of 12.4 mag (290 galaxies), or by 4 σ for the subsample brighter than 11.6 mag (205 galaxies). The square law predictions are in close agreement with direct observation.

The linear law predictions for the dispersion in apparent magnitude are *overestimates*, while any material local perturbations or irregularities would be expected to result in an *underestimate*. The physical reality of exculpatory perturbations or possible evolution is questioned further by the fact that the deviations in the linear law predictions are statistically just as predicted by the square law.

Subject headings: cosmology: observations — distance scale

1. INTRODUCTION

Edwin Hubble was persistently reluctant to accept the hypothesis of the expansion of the universe, notwithstanding that his observations provided both its origin and its putative empirical basis. In a classic joint paper with Tolman (1935) on the nature of the redshift, they wrote (p. 303):

"Until further evidence is available, both the present writers wish to express an open mind with respect to the ultimately most satisfactory explanation of the nebular redshift and, in the presentation of purely observational findings, to continue to use the phrase 'apparent' velocity of recession."

Part II of their paper is entitled "Treatment Assuming Red-shift Not Due to Recession." They write, "As already mentioned, the original Einstein static universe is taken as a suitable model for the case now considered.... Since there would be no systematic motion of the nebulae in such a model, we must assume some other unknown cause for the redshift. In the absence of knowledge as to the mechanism of this cause, we shall take the fractional redshift as proportional to the proper distance to the nebula...." They conclude with the statement (p. 337), "It seemed desirable to express an open-minded position as to the true cause of the nebular redshift, and to point out the indications that spatial curvature may have to play a part in the explanation of existing nebular data."

In 1972, Segal proposed the non-Doppler "chronometric" theory of the redshift, which is precisely along the general lines of the alternative model treated by Hubble & Tolman. It differs, however, from its tentative assumption that the redshift is proportional to the distance, concerning which they write: "Somewhat different laws for the red-shift might perhaps seem more plausible...." This reservation appears to indicate their awareness that curvature effects are locally of second order, which would suggest the variation of the redshift with the square of the distance. The linearity assumption appears to derive from observational findings that they describe as "preliminary" and to have been made for specificity and simplicity.

In the chronometric theory, the redshift varies as the space curvature in the Einstein universe and is locally a homogeneous quadratic function of the distance: $z \sim k^2 d^2$ (or "square" law), where k is the curvature of space and d is the distance in the Einstein universe. The empirical basis of the theory consisted originally of observations on quasars. Their *apparent* extreme luminosity and cutoff in numbers at high redshifts, and other features, were simply explicable without any adjustable cosmological constants or evolution. Moreover, the linear law had been questioned earlier by Hawkins (1964) and was questioned further (independently of the proposal of the chronometric theory) by de Vaucouleurs (1972). The latter, however, ascribed his empirical square law to the putative perturbation of the motions of the galaxies arising from the Local Supercluster.

The issue was not easily resoluble because there was at the time no method for making "hard" cosmological predictions, meaning *objective and reproducible predictions of individual directly observable quantities.* Among these quantities are such cosmologically independent ones as the dispersion in apparent magnitude and the slope of the regression of apparent magnitude on log redshift. There are in addition cosmologically dependent quantities, of which the correlation of absolute magnitude with log redshift, and the dispersion in the absolute magnitude, are among the most familiar.

Thus, the directly observed slope of the magnitude-redshift relation in large eclectic galaxy samples, which were

[1] Massachusetts Institute of Technology, Room 2-244, Cambridge, MA 02139.
[2] Physics Division, IDA, 1801 N. Beauregard Street, Alexandria, VA 22311.

© American Astronomical Society • Provided by the NASA Astrophysics Data System

1996ApJ...465..578S

necessarily cut off in magnitude, was far less than the slope of 5 predicted by the linear law for a fixed luminosity class or random sample of galaxies in space. But this was simply explicable by the progressive magnitude cutoff and a presumed very large dispersion in the intrinsic magnitudes of the sources. Similarly, the correlation of absolute magnitude with log redshift in observed samples was much greater in absolute value than the theoretical value of zero for the population of galaxies in space, but this had a similar explanation.

The difficulty in making "hard" predictions was eliminated by the observation of large objectively selected complete samples on the one hand, and the application of modern statistical methods on the other. Notwithstanding the absence of any a priori knowledge of the luminosity function (LF), or of any cosmology-independent determination of it, probabilistic significance levels could be assessed properly. It became straightforward, if laborious, to make "hard" predictions of any given cosmology and to compare them with direct observation.

The basic first step was the estimation of the LF by efficient and rigorous statistical methods that were subject to a posteriori testing. Traditionally, LF estimates were subjective in part and were not subjected to a posteriori testing. In addition, traditional estimates were based on assumptions regarding the spatial distribution of the source that were not clearly valid, particularly at low redshifts.

The development of a conservative, objective, and a statistically maximally efficient technique for LF estimation, known as ROBUST, altered this situation, soon after large complete samples became available. The ROBUST method and its practical validation and exemplification will be treated in the following section. It will then be applied to a complete optical sample at the lowest redshifts that it presently appears practical to probe, given local peculiar motions and irregularities. The results will include "hard" predictions of the linear and square laws and objective estimates of the probabilistic significance levels of the deviations of the predictions from direct observation. In addition, the predictions of each cosmology for the results of analysis predicated on the other will be determined.

More specifically, the chronometric[3] theory of the redshift (e.g., Segal 1976) presents a challenge to the expanding universe theory that is represented in its most directly observational form by the different predictions of these theories for the magnitude-redshift relation. (The name "chronometric" originates in the inequivalence between the basic notions of time in the Einstein universe, whose space curvature determines the scale of the redshift, and in Minkowski space; see, e.g., Segal & Zhou 1995.) Thus, for a fixed luminosity class, the relation according to Friedmann-Lemaître cosmology (FLC) with $q_0 = 0 = \Lambda$ is

$$m = 5 \log [z(1 + z/2)] + M + C ,$$

where M is the absolute magnitude and C is a conventional constant; according to chronometric cosmology, it is

$$m = 2.5 \log [z/(1 + z)] + M + C .$$

These relations are very different both for large z and for small.

These relations assume implicitly a spectral index $\alpha = 1$ (where larger values of α correspond to softer spectra). For an arbitrary spectral index α, $2.5(1 - \alpha) \log (1 + z)$ must be subtracted from each of the given expressions for m (e.g., McVittie 1965, p. 165). In the present low-redshift regime, the effects of spectral index variations appear inconsequential. Similarly inconsequential are the deviations of the FLC expressions for m from the simple Hubble law expression $m = 5 \log z + M + C$, for values of q_0 and Λ generally considered empirically tenable, and of the chronometric expression from that for a simple square law, $m = 2.5 \log z + M + C$ (see quantitative checks below).

At large z, there is little question that without substantial (redshift-dependent) luminosity evolution, the FLC prediction is inadequate. The phenomenology appears sufficiently clear that this is generally granted, and statistical studies of clearly disinterested data, such as those by Segal & Nicoll (1986, hereafter SN), Segal, Nicoll, & Blackman (1994a), Segal, Nicoll, & Wu (1994b), and Segal & Nicoll (1996), strongly confirm this. These studies indicate, furthermore, that the deviations of the FLC predictions from observation agree with what is predicted by chronometric cosmology. Since redshift-dependent evolution cannot be substantiated by model-independent direct observation, this suggests that it is an artifact of the expanding universe theory (see, e.g., Segal 1986b; Segal et al. 1991).

But in recent years, luminosity evolution has been encroaching on lower and lower redshift regimes. Indeed, Saunders et al. (1990) find both luminosity and density evolution in their analysis of a large *IRAS* sample at redshifts < 0.1. More recently, Segal et al. (1993) find that linear law predictions regarding the flux-redshift relation appear inconsistent with the observations on another large but brighter *IRAS* sample, of average redshift ~ 0.015. (Strauss et al. 1990 and Yahil et al. 1991, in studies of the same data, find no discrepancy from the Hubble law but make no hard predictions of cosmology-independent statistics, and they consider no alternative redshift-distance power laws.) The predictions of the square law are, however, consistent with these observations. This, of course, implies that the linear law predictions will be correct in conjunction with luminosity evolution defined by the difference from the square law.

As in the case of high-redshift observations, the question arises as to whether such evolution can be substantiated observationally. If the linear law is to have nontrivial scientific content, it would appear necessary that at least at sufficiently low redshifts it should hold in its nonevolutionary form. There is a problem in that at such redshifts, local irregularities are relatively likely to perturb the observations and affect the statistics strongly. This problem can, however, be partially circumvented by studying the dispersion in apparent magnitude. All known types of perturbations, or irregularities conceivably arising from known physical mechanisms (other than such as may change the underlying redshift-distance relation), would have the effect of increasing dispersion. Thus, a theoretical prediction of the dispersion in apparent magnitude that neglects such

[3] Briefly, if t is the time in the Einstein universe and x_0 is the time in the covariantly imbedded Minkowski space, then in suitable units $x_0 = 2 \tan \frac{1}{2}(t - t_0)$. Here t_0 is an arbitrary constant, which may, e.g., be taken as 0 at the time of emission or of observation, but not at both. Assuming for specificity the former, then x_0 and t are initially synchronous, but $dx_0 = \sec^2 \frac{1}{2}t\, dt$, so that if a photon is emitted at time 0 and observed at the later time s, its wavelength is increased by the factor $\sec^2 \frac{1}{2}s$, showing that $z = \tan^2 \frac{1}{2}s$.

© American Astronomical Society • Provided by the NASA Astrophysics Data System

1996ApJ...465..578S

local perturbations would therefore be expected to be an *underestimate*. If the prediction is found, however, to be a significant *overestimate*, it can be concluded that the given redshift-distance relation is inconsistent with observation, irrespective of the presence of physically documentable types of perturbations.

This type of analysis has been applied to the cited large *IRAS* galaxy sample. The linear law prediction for the dispersion in log flux is an overestimate that is significant at the level $\sim 10\,\sigma$. Thus, the possible existence of local irregularities is not necessarily a bar to apparently conclusive invalidation of a given proposed magnitude-redshift relation. If, moreover, a very simple alternative law (e.g., without adjustable parameters) is on the one hand itself consistent with the observations, and on the other hand it predicts that the predictions of the linear law will deviate from observation just as observed, it would appear quite improbable that the linear law deviations derive from the scatter caused by the local irregularities.

Visvanathan (1979, hereafter V79), presents a complete, morphologically homogeneous, whole-sky optical sample of about 300 galaxies at very low redshifts. It is an updated version of the classic Shapley-Ames sample (1932), as restricted to the types E, S0, and SB/a. The data of V79 are used here exactly as given in Table 1 of that paper, without any additional corrections for absorption, spectral shape, possible motions of or in the Milky Way, etc.; in particular, the redshifts are heliocentric, modulo adjustment for local motions as specified in V79. In consequence, the present analysis is fully reproducible on the basis of V79 together with the information given here.

A variety of refinements might be contemplated, but they are significantly model dependent, thus impairing the essential cosmology independence and reproducibility of the present analytical frame. Moreover, there is no apparent reason why the relative fit of the redshift-distance laws considered here would be materially altered by the incorporation of such refinements. Indeed, an earlier study by Nicoll & Segal (1982) provides quantitative evidence to the contrary regarding the effects of peculiar motions, the Local Supercluster, the motion of the Galaxy, and clustering. The possible effect of *K*-corrections is estimated below and shown, as expected, to be negligible at the redshifts involved here.

Excluding as usual the regime $cz \leq 500$ km s^{-1} in order to minimize the noise arising from peculiar motions, the sample of V79 has an average redshift ~ 2000 km s^{-1} and a largest redshift ~ 8000 km s^{-1}, at its reported completeness limit of magnitude 12.4. The bright subsample complete to magnitude 11.6 has an average redshift ~ 1600 km s^{-1}, a largest redshift ~ 5000 km s^{-1}, and includes 205 galaxies. The sample appears cosmology independent, well documented, and otherwise appropriate as a database for conducting tests of the linear and square laws in a lower redshift range than has hitherto been reported in detail (but see Nicoll et al. 1980).

V79 itself studied the sample it presented. Corrections to the observed magnitudes were made, primarily on the basis of absolute magnitudes estimated from ultraviolet colors. The "most striking feature" of the resulting Hubble diagram, according to V79, was that the [Hubble line] "fits the distribution of points well" (after the color correction). However, the approach of V79 was quite different from the present one. Thus, V79 did not attempt to predict *directly observed* collective sample statistics, or to estimate objective and reproducible *probabilities of deviations* between prediction and theory. These are, however, what are required for objective statistical validation (subject as always to further observation) by modern scientific standards. Moreover, the only redshift-distance law considered by V79 was the linear one.

In making the present tests, we follow procedures identical to those used earlier, in both optical and other wave bands, that are fully reproducible on the basis of observations as reported and the methodology described here. We treat a variety of subsamples, shown in Table 1, including those defined by the following increasingly conservative magnitude and redshift limits, where c is in units of km s^{-1} and m is the apparent magnitude: (A) $m \leq 12.4$, $cz > 500$; (B) $m \leq 12$, $cz > 500$; (C) $m \leq 11.6$, $cz > 500$; (D) $m \leq 11.6$, $500 < cz \leq 2500$. For each of these subsamples and each cosmology, a nonparametric, statistically optimal estimate of the luminosity function, known as the ROBUST estimate (Nicoll & Segal 1983; see also Segal 1993, Segal et al. 1993), is made. The luminosity functions determine the predictions of the respective cosmologies, and these predictions for directly observable quantities, on the basis of the ROBUST estimates, are compared with the actual observations. This procedure determines statistically appropriate objective estimates of the probabilities that deviations between prediction and observation as large as the actual ones will occur.

In addition to these basic subsamples, we treat secondary ones that deal with particular issues. These subsamples include the brightest apparent magnitude half and the lowest redshift half of sample A; subsamples whose redshifts are constrained to higher values; and samples whose redshifts have been corrected to simulate a possible gravitational effect of the Milky Way. Finally, in the Appendix we treat an alternative luminosity function estimate proposed by a referee on the basis of subcluster considerations.

We use the following abbreviations: The expanding universe and chronometric cosmologies, as represented by the simple low-redshift power-law effective equivalents to the theoretical magnitude-redshift relations cited above, namely,

$$m = (5/p) \log z + M + C_p \quad (p = 1, 2)\,,$$

will be cited as C1 and C2. To facilitate analyses of different cosmologies, C_p will be chosen so that $m = M$ at the typical redshift $cz = 2000$ km s^{-1}, i.e., absolute magnitudes M are defined by the relation $m = (5/p) \log (cz/2000) + M$. The conventional absolute magnitude in the frame of C1 is

TABLE 1

SUBSAMPLES STUDIED

Designation	Defining Constraints	Number of Galaxies
A.....	$cz > 500$, $m \leq 12.4$	290
B.....	$cz > 500$, $m \leq 12.0$	259
C.....	$cz > 500$, $m \leq 11.6$	205
D	$500 < cz \leq 2500$, $m \leq 11.6$	158
E.....	$cz > 1000$, $m \leq 12.4$	249
F.....	$cz > 1500$, $m \leq 12.4$	185
G	$cz > 2000$, $m \leq 12.4$	130
H	$cz > 2500$, $m \leq 12.4$	97
I	$cz > 500$, $m \leq 11.24$	145
J	$500 < cz \leq 1879$, $m \leq 12.4$	146
K	$cz > 500$, $m \leq 11.5$	188

© American Astronomical Society • Provided by the NASA Astrophysics Data System

1996ApJ...465..578S

$M \sim 33$, assuming $H \sim 100$ km s^{-1} at $z \sim 0.01$ in the frame of C1. By luminosity function (LF), we mean here the *normalized* luminosity function, obtained by division of the number of objects in a given absolute magnitude range by the total number, so as to arrive at a probability distribution; this is all that is required for the prediction of the magnitude-redshift relation by ROBUST in a statistically consistent and efficient way (Nicoll & Segal 1983).

We emphasize that *no assumption is made or used here concerning the spatial distribution of the sources.* The only assumption made is that the luminosities of the source population are independent of their redshifts, and that there is no discrimination on the basis of apparent magnitude in the sample selection procedure, down to the designated limiting magnitudes. We treat the following basic directly observable statistics for a given sample:

1. s_m: Dispersion in apparent magnitude;
2. β: Slope of the least-squares regression line for m on $\log z$;
3. ϱ_p: The correlation of absolute magnitude with $\log z$, according to Cp;
4. σ_p: The standard deviation of the residuals in the magnitude-redshift relation, according to Cp.

The ROBUST estimate of the LF that is derived from the sample according to Cp will be denoted as RLFp. On the basis of RLFp, the cosmology-dependent statistics ϱ_p and σ_p can be corrected for the magnitude cutoff (see below or Segal et al. 1993). The corrected values, representing estimates of the source population correlation of absolute magnitude with $\log z$ and its dispersion in absolute magnitude, down to the limit observable in the sample, will be denoted by the superscript "A" (for "after" correction).

In summary, we make three categories of predictions:

1. Directly observable quantities that are *cosmology independent*: s_m and β.
2. Directly observable quantities that are *cosmology dependent*: ϱ_p and σ_p.
3. Quantities that are quasi-directly observable in the sense of being uniquely defined functions of the observed data, but which depend on an estimate of the LF as well as the cosmology: ϱ_p^A and σ_p^A.

These concepts will be illustrated by their application in § 3 to the case of the full sample to the nominal completeness limit of 12.4 mag. Later, the subsamples and variants listed in Table 1 are treated. The arithmetic mean of quantities x will be denoted as $\langle x \rangle$, and the geometric mean will be denoted as $\langle\langle x \rangle\rangle$.

But first we explain and illustrate the origin and application of the LF estimation procedure, ROBUST.

2. NONPARAMETRIC LUMINOSITY FUNCTION ESTIMATION

Nicoll & Segal (1978) presented a method of LF estimation with the following features: (1) it was statistically consistent without any completeness assumption other than the absence of discrimination on the basis of flux, down to a given limiting flux; (2) no assumption concerning the spatial distribution of the sources was required; (3) it was readily susceptible to a posteriori testing; (4) it was of maximal statistical efficiency (here "consistency" and "efficiency" are understood in the sense of the statistical terms introduced by R. A. Fisher). By LF we mean here and hereafter the *normalized* LF, which gives probabilities (totaling unity) or relative frequencies, which as noted above is all that is needed to predict observed quantities that do not depend on the spatial distribution of the sources.

This LF is, of course, not known a priori, but it may be presumed to be describable in terms of suitable unknown parameters. Let these parameters be denoted as θ, and let the differential LF take the form $\phi(M, \theta)$, where M is the absolute magnitude. The method of maximum likelihood is then directly applicable.

More specifically, suppose given a complete sample of limiting magnitude $\bar{m}$, with magnitude and redshift observations $(m_1, z_1), \ldots, (m_n, z_n)$, from a population whose LF takes the form $\phi(M, \theta)$. The likelihood L (e.g., Wilks 1962) can be evaluated as follows: Let the theoretical magnitude-redshift relation take the form $m = M + f(z)$, where $f(z)$ is a given function characteristic of the assumed cosmology. [Thus, $f(z) = 5 \log z + \text{const}$ in the case of the linear law, while $f(z) = 2.5 \log z + \text{const}$ in the case of the square law.] At the redshift z_j, observable objects are limited to those for which $M \leq \bar{M}_j$, where $\bar{M}_j = \bar{m} - f(z_j)$. Let $\Phi(M, \theta)$ denote the cumulative LF: $\Phi(M, \theta) = \int_{-\infty}^{M} \phi(M', \theta)\, dM'$. Taking account of the magnitude limit, the distribution $p(M, \theta)$ of the absolute magnitudes M of objects bright enough to be observed at redshift z_j is $p(M, \theta) = \phi(M, \theta)/\Phi(\bar{M}_j, \theta)$. The likelihood L for the distribution of the absolute magnitudes at the given redshifts is the product $p(M_1) \ldots p(M_n)$, where $M_j = m_j - f(z_j)$. In terms of the directly observed quantities m and z, L takes the form

$$L = \{\phi[m_1 - f(z_1), \theta]/\Phi[\bar{m} - f(z_j), \theta]\} \times \cdots \times \{\phi[m_n - f(z_n), \theta]/\Phi[\bar{m} - f(z_n), \theta]\} .$$

In this form, L is a well-defined function of the observations and of the unknown parameters θ. Maximum likelihood estimation (MLE) consists in taking as the estimate for the unknown parameters θ the values $\hat{\theta}$ that maximize L. Under fairly general conditions (e.g., Wilks 1962) it can be shown that $\hat{\theta}$ exists and that the MLE is of maximal statistical efficiency (asymptotically for large n), in the sense that no other estimate can have smaller expected mean square error. In the most familiar context, the n observations are from identically distributed populations, which is not the case here, but the argument cited is generally applicable.

On occasion the MLE may fail to exist, due to the absence of a maximum for L in the physically realizable parameter range, but for the most part it exists in physically reasonable contexts. Since the physically correct cosmological function $f(z)$ is not known a priori, it is important to conduct an a posteriori test to validate the underlying assumption that the LF has the assumed parametric form $\phi(M, \theta)$. In Nicoll & Segal (1978), a normal law parameterization was used for the bright end of the LF (the only relevant part). This assumption was validated a posteriori in the case of the square law, using a high-efficiency test for normality of a population whose parameters were estimated from the data used to validate the normality assumption. In the case of the linear law, however, the normal law parameterization was rejected by the a posteriori test. This was virtually inevitable for any power law that differs greatly from the square law, since the power itself had earlier been estimated by MLE and found to approximate 2.

Thus, it appeared that an arbitrary cosmological function $f(z)$ could avoid rejection relative to any specific analytical

© American Astronomical Society • Provided by the NASA Astrophysics Data System

1996ApJ...465..578S

parameterization of the unknown LF by arguing that the true physical LF did not necessarily conform to the assumed parameterization. Fortunately, this problem could be overcome by the development of a method in which no specific parameterization is made. Instead, the LF is represented by a histogram (or step function), as frequently done in practice, and the heights of the histogram rectangles (or the values of the step function) determined by MLE in Nicoll & Segal (1980, 1983). A closed form expression for the MLE, requiring only recursive algebra, was obtained. This procedure, known as ROBUST, has since been applied to a variety of complete samples, in several wave bands; see, e.g., Segal (1989, 1993), and Segal et al. (1993, 1994a, b). The same basic nonparametric approach may also be applied by "brute force" computations to maximize the expression for the likelihood, as done later by Saunders et al. (1990); however, this procedure does not necessarily ensure that a maximum actually exists.

The essential idea of ROBUST is quite natural and simple. Suppose that a complete sample is observed in which there are only two different redshifts, z and z', where $z < z'$. At the redshift z (respectively, z'), the observable absolute magnitudes are those brighter than $\bar{m} - f(z) = \bar{M}$ (respectively, $\bar{M}'$), say. Suppose there are s sources at redshift z and a' at redshift z'. All the a sources at redshift z are brighter than $\bar{M}$, while of the a' sources at redshift z', some (say b in number) will be brighter than $\bar{M}$ and some (say c in number) will have absolute magnitudes M in the range $\bar{M} < M \leq \bar{M}'$. All information regarding the LF in the range brighter than $\bar{M}$ is obtained by combining the a sources at redshift z with the b sources at redshift z' of absolute magnitude brighter than $\bar{M}$. This then determines in the usual way a frequency distribution in this range, i.e., observed number in a bin divided by the total number. All information regarding the LF in the absolute magnitude range from $\bar{M}$ to $\bar{M}'$ is contained in the subsample of c sources, which mean then determines a frequency distribution in this range.

At this point, one has two normalized frequency distributions, one in the range brighter than $\bar{M}$, and the other in the range between $\bar{M}$ and $\bar{M}'$. The problem is now to obtain the best estimate of the normalized frequency distribution representing the LF in the range brighter than $\bar{M}'$. This requires an estimate of the relative frequencies in the two ranges. The only information in the sample concerning this is in the sample brighter than $\bar{M}'$, which indicates that the relative frequency of the two absolute magnitude ranges is $b:c$. This leads to the conclusion that if the LF restricted to the brighter range is $\psi(M)$ and that restricted to the fainter range is $\psi'(M)$, then the best estimate for the LF in the combined range is $\phi(M) = [b\psi(M) + c\psi'(M)]/(b + c)$.

This is the root idea of ROBUST, and the procedure may now be extended recursively to the case of any number of distinct redshifts. The method adapts simply in principle to the case in which the limiting magnitude varies with the redshift or sky position of the object, to the case of a progressive apparent magnitude dependent cutoff, etc. These refinements, however, are not needed in the present paper.

The expression for the ROBUST estimate $\hat{\phi}(M)$ of the LF $\phi(M)$ is then a rational function of the occupation numbers of absolute magnitude intervals. The ratios of these occupation numbers are involved, and on occasion the vanishing of one or more denominators signals the nonexistence of the MLE, but in practice this happens only for very small samples and/or poorly fitting cosmologies. No such singular samples are involved in the present analysis.

The computer implementation of ROBUST used here is identical to that used in all our comparative cosmological studies during the past decade. Each cosmology tested is allowed the same number of adjustable parameters, namely 10, to describe the part of the observed absolute magnitude range subject to variable cutoff. This determines the equal-sized binning. After making the ROBUST estimate, the binning is standardized by interpolation for convenience in making numerical integrations, Monte Carlo simulations, etc., here (as earlier) into bins of size 0.25 mag. Using numerical integration, the correlation of absolute magnitude with redshift, the standard deviation, and mean of the absolute magnitudes may be corrected for the magnitude cutoff ("Malmquist") bias by subtraction from each observed absolute magnitude of its expectation value according to the ROBUST LF for objects at its observed redshift (see, e.g., Segal et al. 1993 for the analytic expressions).

The most crucial feature of an estimation method is its statistical consistency (in the sense of Fisher), meaning that asymptotically as the sample size increases indefinitely, the estimate converges to the true value. A highly desirable feature is statistical efficiency, meaning that the speed of convergence of the estimate to the true value is maximal (or equivalently, that asymptotically, at least, all the information in the observations regarding the parameters θ being estimated is used). Under normally regular conditions, the MLE has both these features (e.g., Wilks 1962). An additional desirable feature, which, however, is generically absent, is that of statistical sufficiency, meaning that even in finite samples, all information regarding θ is contained in the estimate $\hat{\theta}$. (In other words, the conditional distribution of the observations given $\hat{\theta}$ is independent of the unknown parameter θ). Fortunately, ROBUST has all these features.

Given a cosmology and the LF, the hard predictions regarding a complete sample of designated limiting magnitude $\bar{m}$ are mathematically uniquely determined. However, even in simple parametric cases the requisite mathematical analysis is often burdensome. A more practical method of making hard predictions, which is at the same time astronomically more intelligible and intuitive, is via Monte Carlo analysis. In the present usage, this is based on the construction of a number N of samples, set up by random selection from the LF, subject to the given limiting magnitude, and placed at the n observed redshifts; e.g., the redshifts z may be arranged in increasing order and an absolute magnitude M drawn at random from the LF. The corresponding object at redshift z would have apparent magnitude $m = M + f(z)$, where $f(z)$ is determined by the cosmology. If m is fainter than the limit $\bar{m}$, the selected absolute magnitude is rejected, and another selection is made. This process is repeated until an object that would be as bright or brighter than $\bar{m}$ is selected. The next redshift is then treated in the same way, etc.

For each of the N random samples obtained in this way, various statistics including the basic directly observable ones are computed. For any given statistic, e.g., the slope β of the magnitude-redshift regression line, the mean $\pm$ the standard deviation of the N predictions represents the prediction of the given cosmology. This is then subject to comparison with the directly observed value. An objective and reproducible estimate of the probability of a deviation as

© American Astronomical Society • Provided by the NASA Astrophysics Data System

1996ApJ...465..578S

large as that observed can also be made, e.g., the probability is estimated to be less than $1/N$ if the observed deviation exceeds that in all the N random samples. In principle, these estimates are subject to random fluctuations in view of the Monte Carlo method employed, but they are entirely well defined mathematically, and in practice, in samples of the size and signal-to-noise ratio quality of the present one, these fluctuations are inconsequential.

The validity of ROBUST at the level of practical astronomy, and as programmed, is demonstrated repeatedly by the application of the Monte Carlo method just described. Invariably, the random samples constructed assuming C1 predict that statistics are in close internal agreement with C1 and inconsistent with those of C2; and vice versa; e.g., the C1-predicted values for its bias-corrected correlation ϱ_1^A of absolute magnitude with redshift approximates zero, while the corresponding prediction for ϱ_2^A is significantly different from zero, and vice versa. Moreover, the sufficiency of the procedure from the standpoint of numerical analysis is shown by the striking accuracy of many of the predictions, e.g., those of σ_p for either cosmology (see, e.g., Tables 2–5).

Traditionally, an important method of LF estimation has been based on analysis of clusters or groups of galaxies thought to be at the same redshift, within presumptively negligible peculiar effects. Since there is no model-independent means of separating the universal cosmic redshift effect from the effects of peculiar motions, and definitive exclusion of foreground or background objects is not possible, the validity of accuracy of this method is arguable. A referee has kindly supplied LF estimates of this type based on a subsample of V79. This estimate shows some differences from the ROBUST estimates. The cluster-based estimate for the linear law and its hard predictions are reported in the Appendix.

3. FULL SAMPLE ANALYSIS

The application of the statistical method described above will now be exemplified by analysis of sample A within the respective frames of the linear and square laws. The C1 and C2 ROBUST LFs (denoted as RLF1 and RLF2) are shown in Figures 1 and 2. Table 2 compares the theoretical predictions, where here and throughout this work we use $N = 100$ random samples for the Monte Carlo analysis, on the basis of RLF1 and RLF2 with the actual observed values. The errors shown on the right are in units of the standard deviations shown in the middle columns. Note that the C1 standard deviations are typically significantly larger than the C2 standard deviations.

TABLE 2

STATISTICAL ANALYSIS OF THE SUBSAMPLE WITH $m \leq 12.4$, $cz > 500$ (290 GALAXIES; $\langle cz \rangle = 2200$; $\langle\langle cz \rangle\rangle = 1891$; $cz_{max} = 8053$)

STATISTIC	OBSERVED VALUES	PREDICTED VALUES		ERRORS	
		C1	C2	C1	C2
s_m	0.75	1.05 ± 0.04	0.78 ± 0.03	7.3	1.1
β	1.77	2.71 ± 0.19	1.93 ± 0.15	4.9	1.1
ϱ_1	−0.78	-0.55 ± 0.04	-0.76 ± 0.02	6.0	1.1
σ_1	0.98	0.99 ± 0.03	0.96 ± 0.03	0.3	0.2
ϱ_2	−0.27	0.06 ± 0.05	-0.21 ± 0.05	6.1	0.1
σ_2	0.64	0.83 ± 0.03	0.64 ± 0.03	6.2	0.1
ϱ_1^A	−0.30	0.00 ± 0.05	-0.28 ± 0.4	6.3	0.6
σ_1^A	1.04	1.06 ± 0.05	1.00 ± 0.06	0.4	0.6
ρ_2^A	−0.05	0.31 ± 0.04	-0.01 ± 0.05	7.9	0.7
σ_2^A	0.69	0.87 ± 0.4	0.69 ± 0.03	5.2	0.6

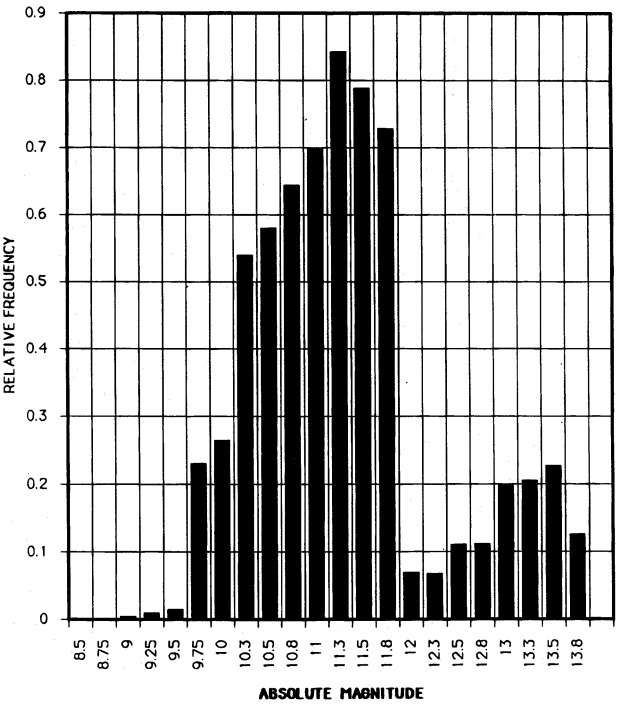

FIG. 1.—Differential RLF1 for sample A

To illustrate the procedure used, Figure 3 provides a more precise version of the predictions of s_m in the 100 random samples. It consists of histograms showing the distributions of the predicted values according to C1 and C2. Figure 4 does the same for the ϱ_p and also includes cross predictions of each cosmology for the results of analysis predicated on the other. The figures provide graphic indica-

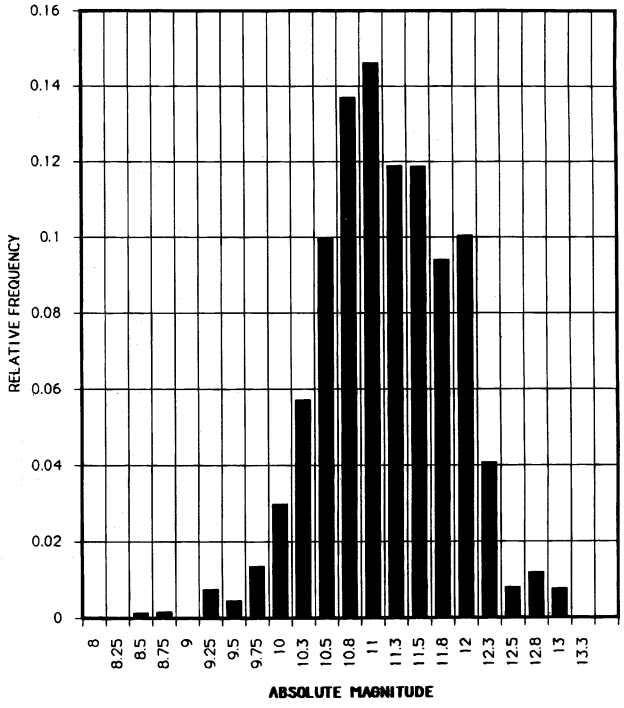

FIG. 2.—Differential RLF2 for sample A

© American Astronomical Society • Provided by the NASA Astrophysics Data System

1996ApJ...465..578S

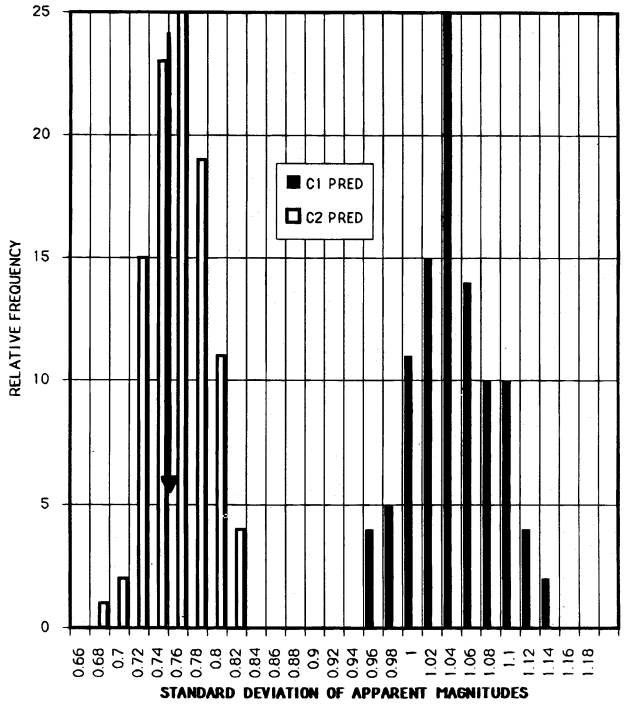

FIG. 3.—Distribution of the Cp predictions ($p = 1, 2$) for the dispersion in apparent magnitude in sample A. Arrow shows the observed value.

tions of the deviance of the C1 and the consistency of the C2 predictions; note also that the C2 prediction for ϱ_1 is far more accurate than that of C1 itself.

In summary, Table 2 indicates considerable inconsistency for the C1 predictions of directly observable quantities. The most damaging inconsistency is the large C1 overestimate for s_m, which as noted appears inexplicable by ancillary perturbations of any physically known type, other than such as may change the linear law itself. To be sure, a displacement of the linear law toward the square law would improve the fit of its predictions, and if sufficiently large it will remove its apparent inconsistency, as a consequence of the consistency of C2. It might be argued that local gravitational effects arising from local overdensity could effectively give rise to such a displacement, and we examine later the possible effects of a displacement of a physically tenable order of magnitude.

In addition, C1 is unable to predict consistently the observed correlation between the C1 absolute magnitude and redshift. The notably large absolute value of this correlation raises the question of whether the magnitude cutoff can be an adequate explanation. The observed value is far greater in absolute value than the C1 predicted value. The C1 prediction for the slope of the magnitude-redshift regression line is less deviant, although still significantly so, while its prediction for the dispersion of the residuals in the redshift-magnitude relation is consistent with the observed value. The relative sensitivity of these four statistics seen here is similar to that found in other samples, e.g., the *IRAS* samples treated in Segal & Nicoll (1992) and Segal (1993).

In contrast, the C2 predictions for these statistics are quite consistent with observation. Moreover, the C2 predictions for the C1 correlation and dispersion of residuals are entirely consistent with the observed values, notwithstanding that C1 is unable to predict this correlation consistently. On the other hand, C1 is quite unable to explain the good fit of the C2 predictions. It predicts that the standard deviations of the C2 residuals will be much larger than they actually are, and its deviant prediction for the C2 correlation indicates that after correction for the magnitude cutoff, there will remain a large nonzero correlation between C2 absolute magnitudes and the redshifts. The vanishing of ϱ_2^A within statistical fluctuations shows that this is not the case, as discussed next.

The situation is similar in the cases of the statistics that depend on an estimate of the LF. Corresponding to their putative statistical consistency, both C1 and C2 predict that, after correction for the observational cutoff bias, their

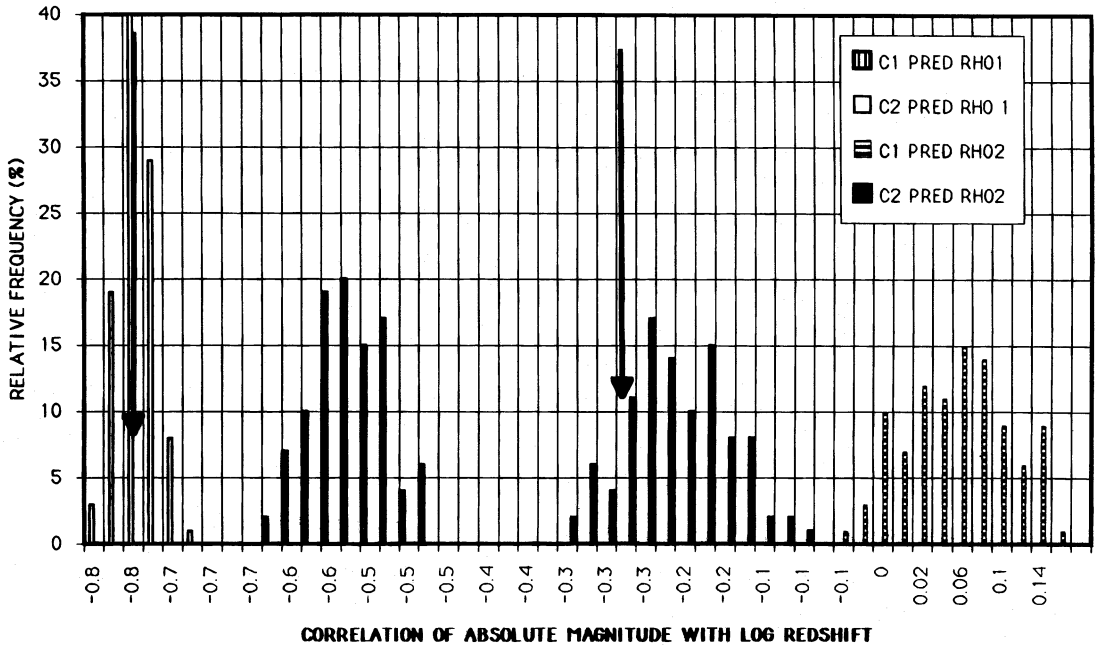

FIG. 4.—Distributions of the Cp predictions for the correlations of absolute magnitude with log redshift ($p = 1, 2$) in sample A. Arrows show the observed values (for C1 on the left and C2 on the right).

© American Astronomical Society • Provided by the NASA Astrophysics Data System

1996ApJ...465..578S

respective correlations of absolute magnitude with redshift will approximate zero. However, only in the case of C2 is this prediction actually correct. As regards the cross predictions, C1 predicts that C2 will fit poorly, as evidenced by its predictions of large values for $|\varrho_2^A|$ and σ_2^A, which however are by no means attained. In contrast, the predictions of C2 for ϱ_1^A and σ_1^A are accurate.

Thus, the apparent deviations of the predictions of the nonevolutionary Hubble law from observation in a redshift regime averaging about 2000 km s^{-1} is comparable to that at much higher redshifts, as measured by probabilistic significance levels. Chronometric cosmology (CC) provides a common explanation for these apparent serious flaws. However, rigorous estimation of an LF is necessarily predicated on a completeness assumption, here to the effect that the sample treated is complete to the limiting magnitude of 12.4. There is no special reason to believe that it is not, but it is in the nature of incompleteness that it is not directly observable and has uncertain potential. Accordingly, conservative testing requires analysis of bright subsamples, involving a trade-off between sample size and greater assurance of completeness.

4. ANALYSIS OF BRIGHT SUBSAMPLES

First we treat two bright subsamples, successively brighter by 0.4 mag than the full sample. Table 3 summarizes the analysis of the subsample with magnitude limit 12, on the same basis as Table 2.

In summary, Table 3 indicates that C1 is inconsistent with the observations, at a somewhat lower level of significance than in the case of Table 2. This reduction in significance is, however, no more and perhaps less than might be expected from the combination of a smaller size sample with a lesser dynamic range. There is no indication that incompleteness was a factor in the rejection of C1 by Table 2. The fit of C2 is closer than in the case of Table 2, while if incompleteness were a factor in the consistency of C2 indicated by Table 2, it would be expected that the enhanced completeness of the brighter subsample would show larger deviations for C2, or at least not lead to a closer fit.

On the other hand, incompleteness remains a conceivable factor in the subsample brighter than magnitude 12 as well as in the full sample. It would seem quite surprising, however, if there were any material incompleteness at the quite bright limiting magnitude 11.6. Table 4 summarizes the results of analysis of this subsample, on the same basis as earlier.

TABLE 3

STATISTICAL ANALYSIS OF THE SUBSAMPLE WITH $m \leq 12$, $cz > 500$
(257 GALAXIES; $\langle cz \rangle = 2051$; $\langle\langle cz \rangle\rangle = 1779$; $cz_{max} = 7015$)

STATISTIC	OBSERVED VALUES	PREDICTED VALUES C1	PREDICTED VALUES C2	ERRORS C1	ERRORS C2
s_m	0.68	0.92 ± 0.04	0.70 ± 0.03	6.0	0.5
β	1.558	2.18 ± 0.17	1.635 ± 0.148	3.7	0.5
ϱ_1	−0.81	-0.64 ± 0.03	-0.796 ± 0.0219	5.1	0.5
σ_1	0.98	1.01 ± 0.03	0.974 ± 0.0297	1.0	0.3
ϱ_2	−0.35	-0.10 ± 0.05	-0.320 ± 0.0538	5.0	0.6
σ_2	0.62	0.78 ± 0.03	0.622 ± 0.0289	5.0	0.1
ϱ_1^A	−0.01	-0.19 ± 0.04	-0.00 ± 0.04	3.1	1.6
σ_1^A	1.01	1.06 ± 0.05	0.97 ± 0.05	0.9	1.8
ϱ_2^A	0.00	0.25 ± 0.04	-0.01 ± 0.05	6.1	0.2
σ_2^A	0.67	0.83 ± 0.04	0.67 ± 0.03	4.5	0.0

TABLE 4

STATISTICAL ANALYSIS OF THE SAMPLE WITH $m \leq 11.6$, $cz > 500$
(205 GALAXIES; $\langle cz \rangle = 1823$; $\langle\langle cz \rangle\rangle = 1616$; $cz_{max} = 5027$)

STATISTIC	OBSERVED VALUES	PREDICTED VALUES C1	PREDICTED VALUES C2	ERRORS C1	ERRORS C2
s_m	0.62	0.78 ± 0.04	0.62 ± 0.04	4.0	0.1
β	1.34	1.92 ± 0.23	1.35 ± 0.19	2.5	0.0
ϱ_1	−0.82	-0.71 ± 0.03	-0.82 ± 0.02	3.6	0.0
σ_1	0.95	0.94 ± 0.03	0.96 ± 0.04	0.5	0.0
ϱ_2	−0.41	-0.19 ± 0.06	-0.41 ± 0.06	3.4	0.1
σ_2	0.60	0.68 ± 0.03	0.61 ± 0.04	2.3	0.1
ϱ_1^A	−0.08	-0.01 ± 0.05	-0.14 ± 0.04	1.6	1.5
σ_1^A	0.93	0.97 ± 0.04	0.93 ± 0.05	0.9	0.1
ϱ_2^A	0.05	0.21 ± 0.05	-0.02 ± 0.06	3.2	1.1
σ_2^A	0.66	0.73 ± 0.04	0.66 ± 0.04	2.1	0.0

As in the case of Table 3, Table 4 shows no sign that incompleteness may be a factor in the rejection of C1 by the observations treated in Table 2. On the contrary, the fit of C2 is remarkably close, in its predictions of the C1 statistics, as well as its own and the cosmology-independent statistics s_m and β. Rather than improving in fit in the lower redshift regime, C1 shows large deviations relative to sample size in the two major statistics s_m and ϱ_1. Thus, even by very conservative standards, there is little apparent question that the nonevolutionary form of C1 is inconsistent wth direct observations in the redshift regime treated here.

It could perhaps be argued that although this regime has an average redshift ~ 2000 km s^{-1}, the higher redshifts in the subsample perturb the results significantly. To reject rigorously the nonevolutionary Hubble law in a very low redshift regime, using a sample of rather unexceptionable completeness, we treat also the subsample of limiting magnitude 11.6 in the redshift range $500 < cz \leq 2500$. Table 5 summarizes the results of analysis on the same basis as earlier.

Table 5 shows the same inconsistencies of the C1 predictions with observation as earlier, without any indication whatsoever for a closer fit at the very lowest redshifts. The predictions of C2 remain entirely consistent with the observations, but they do not fit quite as well as in the earlier samples, as might have been expected from the impact of local irregularities, such as Virgo.

Thus, it appears necessary to adjust the classical linear law in order to achieve consistency between theory and observation, by evolution of some type or other ancillary hypotheses. On the other hand, the predictions of C2 for the

TABLE 5

STATISTICAL ANALYSIS OF THE SUBSAMPLE WITH $m \leq 11.6$,
$500 < cz \leq 2500$ (158 GALAXIES; $\langle cz \rangle = 1409$;
$\langle\langle cz \rangle\rangle = 1325$; $cz_{max} = 2488$)

STATISTIC	OBSERVED VALUE	PREDICTED VALUES C1	PREDICTED VALUES C2	ERRORS C1	ERRORS C2
s_m	0.63	0.78 ± 0.05	0.66 ± 0.04	3.3	0.8
β	1.12	2.14 ± 0.39	1.43 ± 0.32	2.7	0.8
ϱ_1	−0.71	0.54 ± 0.56	-0.67 ± 0.04	3.1	1.0
σ_1	0.85	0.85 ± 0.04	0.83 ± 0.04	0.2	0.5
ϱ_2	−0.34	-0.09 ± 0.08	-0.26 ± 0.07	3.0	1.1
σ_2	0.64	0.72 ± 0.4	0.64 ± 0.04	1.9	0.1
ϱ_1^A	−0.20	-0.03 ± 0.05	-0.19 ± 0.05	3.3	0.1
σ_1^A	0.89	0.91 ± 0.04	0.93 ± 0.06	0.5	0.7
ρ_2^A	−0.07	0.16 ± 0.06	-0.02 ± 0.07	3.7	0.6
σ_2^A	0.70	0.76 ± 0.39	0.70 ± 0.04	1.4	0.0

© American Astronomical Society • Provided by the NASA Astrophysics Data System

1996ApJ...465..578S

values of the cosmology-dependent statistics expected from analysis predicated on C1 are in very good agreement with the actual values of these statistics. This suggests that such hypothetical perturbations to the linear law may lack physical reality. To examine this possibility more closely, the predictions of C2 for the values of the cosmology-independent quantities s_m and β that are predicted by C1 via the construction of random samples drawn from its estimated LF will be determined. Such predictions could not be made above because inevitably the values of these statistics obtained in random samples constructed assuming C2 do not involve any cosmology other than C2. An intermediate step is required, namely, the estimation of the C1 LF by C2. The next section treats this and other aspects of the LF estimation.

5. A POSTERIORI TESTS OF THE LFs

Given (*a*) the correct cosmology, (*b*) the correct LF, and (*c*) a specific set of redshifts, the RLF for any other cosmology when applied to a sample of given redshifts is mathematically uniquely determined. In particular, the assumption that C1 (or C2) is correct, together with RLF1 (or RLF2), and the observed sample redshifts, determine uniquely an estimate of the LF for any *other* cosmology.

A natural and practical way to estimate such LFs, which is also statistically consistent, proceeds by adaptation of the bootstrap Monte Carlo method used above. Suppose that N random samples are made, drawn from the RLF for cosmology A for a given sample, and placed at the observed redshifts, consistently with the given limiting magnitude. Cosmology B can be applied to the ROBUST analysis of each such artificial sample, thereby obtaining from each sample an estimate of the RLF of cosmology B. The arithmetic average of these N estimates of the LF converges, as N increases indefinitely, to the LF for cosmology B predicted by cosmology A.

If $A = Cp$ and $B = Cq$, then the resulting estimate will be denoted as RLF(q, p); this is a stochastic quantity, and so it lacks the absolute unicity of the RLFp. Thus, RLF(q, p) represents an appropriate estimate of RLFq under the assumption that Cp is correct. If now the random sample construction used above is applied to RLF(q, p), instead of to RLFq, it represents a statistically consistent prediction by Cp (under the assumption of its correctness) of the results of analysis predicated on Cq, for cosmology-independent quantities as well as those whose analysis involves assumption of cosmology q. In particular, this procedure provides estimates of the C1 predictions for s_m and β, under the assumption that C2 is correct, and vice versa. In addition, it provides estimates of the cosmology-dependent quantities, which may be checked for consistency with those obtained more directly, and reported in Tables 2–5.

The total absolute deviation A[RLFp, RLF(p, p)] between RLFp and the self-prediction RLF(p, p) (i.e., the total variation of the difference between the two probability distributions) is considerably larger when $p = 1$ than when $p = 2$, by a factor of more than 2.5. Table 6 gives the values of all of the respective A[RLFp, RLF(p, q)] for samples A and D.

On the basis of the C2 estimate RLF(1, 2) of RLF1, predictions can be made by C2 of the results of random sample analyses predicated on C1. The basic results for sample A are summarized in Table 7; the corresponding results for the magnitude cutoff bias–corrected statistics are quite similar and are omitted. The standard errors of the errors shown in the column on the right are the square roots of the sums of squares of the errors of C1 prediction shown in Table 2 and of C2 estimation for the present predictions.

TABLE 6

VALUES OF A[RLFp, RLF(p, q)] FOR SAMPLES A AND D

	Sample A		Sample D	
q	$p = 1$	$p = 2$	$p = 1$	$p = 2$
1.....	0.043	0.087	0.044	0.058
2.....	0.068	0.016	0.079	0.018

Table 7 shows that C2 estimates correctly the results of predictions predicated on C1, for the basic statistics treated here. It indicates thereby that the deviations of the C1 predictions from observation are identical, within statistical fluctuations, with what would be expected if C2 were correct. This, in turn, indicates that the evolution hypothesis is supererogatory and merely exculpatory.

Confirmation for this conclusion is provided by the results of the similar analysis for sample D, which are summarized in Table 8. Table 8 is qualitatively quite similar to Table 7. It indicates that even for the brightest galaxies in the lowest redshift range, the deviations of the C1 predictions from direct observation are statistically just as implied by C2. There is no indication whatsoever for any substantial source for the deviations, other than the simple difference between the C1 and C2 redshift-distance relations.

6. MUTUAL CONSISTENCY OF LFs

A sample that is complete to a given magnitude is automatically complete to any brighter magnitude, and in consequence the LFs for the sample and bright subsamples should be mutually consistent. They need not be identical apart from statistical fluctuations, since a bright subsample may sample a more limited absolute magnitude range than the full sample. However, when the LFs of bright sub-

TABLE 7

PREDICTIONS OF C2 FOR THE RESULTS OF RANDOM SAMPLE ANALYSES ASSUMING C1, FOR THE SUBSAMPLE WITH $m \leq 12.4$, $cz > 500$

Statistic	Actual C1 Prediction	C2 Estimate of C1 Prediction	Error in C2 Estimate of C1 Prediction
s_m	1.05 ± 0.04	1.08 ± 0.04	0.02 ± 0.06
β	2.70 ± 0.19	2.86 ± 0.18	0.16 ± 0.26
ϱ_1	-0.55 ± 0.04	-0.53 ± 0.04	0.02 ± 0.05
σ_1	0.99 ± 0.03	0.97 ± 0.03	0.03 ± 0.05
ϱ_2	0.06 ± 0.05	0.10 ± 0.050	0.04 ± 0.07
σ_2	0.83 ± 0.03	0.83 ± 0.04	0.00 ± 0.05

TABLE 8

PREDICTIONS OF C2 FOR THE RESULTS OF RANDOM SAMPLE ANALYSES ASSUMING C1, FOR THE SUBSAMPLE WITH $m \leq 11.6$, $500 < cz \leq 2500$

Statistic	Actual C1 Prediction	C2 Estimate of C1 Prediction	Error in C2 Estimate of C1 Prediction
s_m	0.78 ± 0.05	0.81 ± 0.05	0.02 ± 0.07
β	2.14 ± 0.39	2.40 ± 0.37	0.26 ± 0.54
ϱ_1	-0.54 ± 0.06	-0.49 ± 0.06	0.05 ± 0.08
σ_1	0.85 ± 0.05	0.83 ± 0.05	0.03 ± 0.06
ϱ_2	-0.09 ± 0.08	0.02 ± 0.08	0.07 ± 0.12
σ_2	0.72 ± 0.04	0.72 ± 0.04	0.00 ± 0.06

© American Astronomical Society • Provided by the NASA Astrophysics Data System

1996ApJ...465..578S

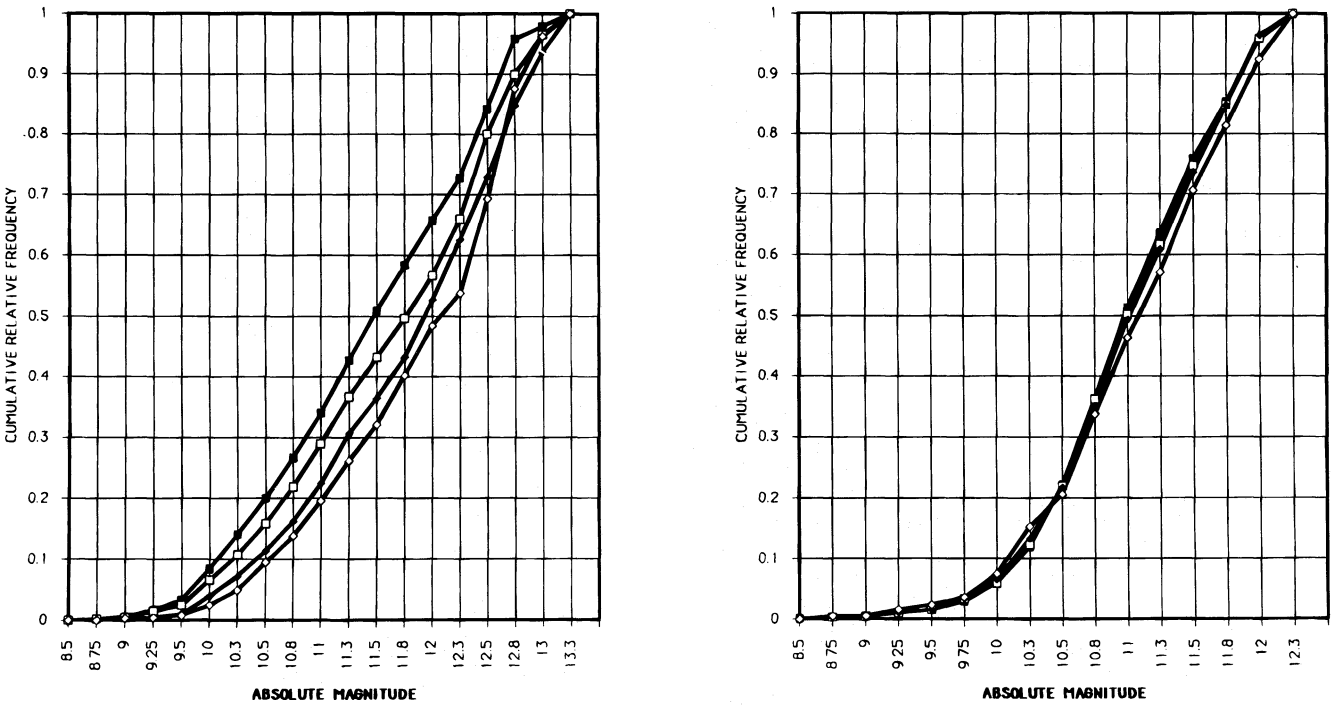

FIG. 5.—*Left*: cumulative C1 luminosity functions of samples A–D in their common range. *Filled squares*, RLF 1; *open squares*, RLF (1, 1); *filled diamonds*, RLF (1, 2). *Right*: Cumulative C2 luminosity functions for samples A–D in their common range. *Filled squares*, RLF2; *open squares*, RLF (2, 2); *filled diamonds*, RLF (2, 1).

samples are restricted to a common range and normalized to a probability of one over this range, they are predicted to be in statistical agreement, if the assumed cosmology is correct.

In the cases of samples A–D, little normalization is required. Assuming C1, the range up to absolute magnitude $M = 13.5$ is included in RLF1 for all the samples. For sample A, this range includes the fraction 0.965 of RLF1; for sample B, it includes the fraction 0.976 of RLF1; for samples C and D, it includes the entire range of the RLF1's. The RLF1's may accordingly be compared properly by renormalizing the RLF1 for samples A and B by cutoffs in the RLF1 given above after the absolute magnitude 13.25 in the column on the left, i.e., after the bin 13.25–13.5, followed by divisions by the respective fractions noted. A similar procedure applies in the case of C2. The resulting comparable LFs are shown in Figure 5.

The C1 LFs did not appear to be mutually consistent. In terms of the Kolmogorov-Smirnov statistic D, or maximum difference between the cumulative distributions $D(A, C) = 0.15$ and $D(A, D) = 0.19$, where the RLF for sample X is denoted simply as X. In contrast, in the case of C2, $D(A, C) = 0.03$ and $D(A, D) = 0.06$. While no precise significance level is assigned to these deviations, since the samples in question are not independent, the exponential dependence on D of the asymptotics for this statistic in the statistically independent case [probability of a deviation as large as $D \sim 2 \exp(-2nD^2)$, where n is the sample size] is indicative on an order-of-magnitude basis of mutual inconsistency in the case of C1, but consistency in the case of C2.

More specifically, the C1 LFs show a brightward trend as the defining constraints for the sample are lessened, or in effect, they show apparent evolution brightward as the redshift increases. No such trend appears in the case of C2. Quantitatively, the estimated mean absolute magnitudes for the samples, as corrected for the magnitude cutoff bias using the RLFs, are shown in Figure 6. We note that this apparent evolutionary trend, according to which higher redshift objects appear brighter, is similar to that in quasar samples when analyzed according to FLC.

7. SIGNIFICANCE OF GRAVITATIONAL PERTURBATIONS

The foregoing analysis has used a variety of objective tests to probe the absolute and comparative capacity of C1

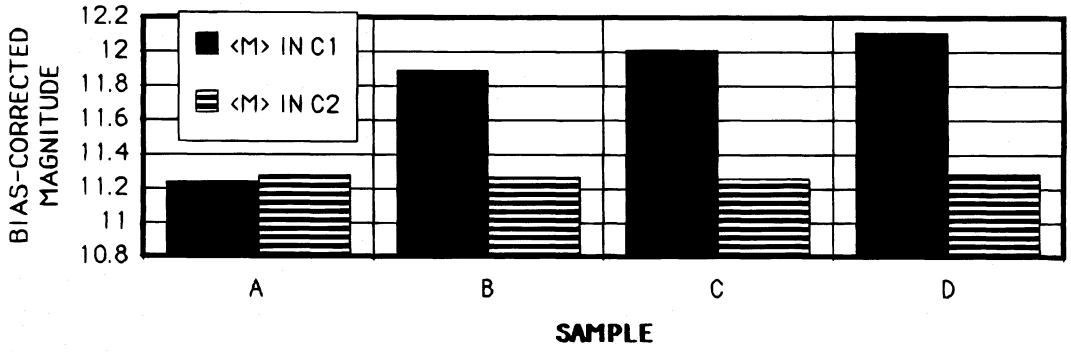

FIG. 6.—The mean absolute magnitudes of samples A–D after correction for the magnitude cutoff bias, as a function of redshift

© American Astronomical Society • Provided by the NASA Astrophysics Data System

1996ApJ...465..578S

and C2 to fit the magnitude-redshift relation at very low redshifts. There appears to be little question that C1 is inconsistent with the sample observations, in a number of important respects. These inconsistencies can hardly be ascribed to physically known types of perturbations. These would lead to an underestimate of the dispersion in apparent magnitudes, rather than the actual large excess of the C1 prediction over observation. Moreover, it is difficult to conceive of a perturbation whose effects would simulate, in the whole sky, those implied by the simple substitution of C2 for C1. But C2 predicts that the C1 predictions will deviate in just the way that is actually observed.

As noted earlier, it may be argued that the local overdensity due to the Galaxy, or that an extraordinary local irregularity, might perturb the local redshift-distance relation, thereby producing an apparent but specious deviation of observation from the predictions of the unperturbed Hubble law. That neither of these is the case can be checked in two ways. First, the subsample at higher redshifts would be affected less by the assumed local gravitational effect or irregularity. The C1 predictions on the basis of this subsample would accordingly be expected to be increasingly consistent with the observations in subsamples in increasingly higher redshift regimes. However, they are no less and perhaps more deviant than those in the lower redshift regime, while at the same time the C2 predictions are in slightly closer agreement with observation than in the case of the full sample. Tables 9–12 show the results of the same analysis as earlier, as applied to the subsamples D–G.

The distributions of the predicted statistics, as well as the statistics themselves, are similar to those for samples A–D. This is exemplified more fully for the subsample at redshifts >2000 km s^{-1} by Figures 7 and 8, which show the distributions of s_m and the ϱ_p on the same basis as Figures 3 and 4. Apart from the impact of a smaller sample size and a lesser dynamic range, the higher redshift results are qualitatively identical to those for the full sample.

Second, it remains to treat the possible effect of an adjustment motivated by the hypothesis that the overdensity of the Milky Way region may cause local redshifts to lag behind the actual distances. As noted by V79, "The existing claims for the local velocity deviations are varied and controversial ... the question of whether gravitational effects due to density excessses produce a measurable component in the velocity axis is yet to be answered." At the present time, the claim that the latter is the case has yet to be substantiated in any model-independent way.

However, to give the hypothesis the benefit of the doubt, an assessment of the impact of such gravitational effects may be obtained by the addition of an appropriate correction to the observed redshifts. In its simplest form this correction may be approximated as a fixed amount, which may

TABLE 9

STATISTICAL ANALYSIS OF THE SAMPLE WITH $cz > 1000$, $m \leq 12.4$ ($N = 249$; $\langle cz \rangle = 2426$; $\langle\langle cz \rangle\rangle = 2171$; $cz_{max} = 8053$)

STATISTIC	OBSERVED VALUE	PREDICTED VALUES C1	PREDICTED VALUES C2	ERRORS C1	ERRORS C2
s_m	0.70	0.92 ± 0.04	0.70 ± 0.03	6.0	0.3
β	1.87	2.76 ± 0.18	1.82 ± 0.17	5.1	0.3
ϱ_1	−0.72	-0.53 ± 0.04	-0.73 ± 0.03	5.0	0.3
σ_1	0.87	0.86 ± 0.04	0.87 ± 0.03	0.1	0.1
ϱ_2	−0.21	0.06 ± 0.06	-0.22 ± 0.05	4.6	0.3
σ_2	0.61	0.74 ± 0.03	0.61 ± 0.03	4.1	0.1

TABLE 10

STATISTICAL ANALYSIS OF THE SUBSAMPLE WITH $cz > 1500$, $m \leq 12.4$ ($N = 185$; $\langle cz \rangle = 2832$; $\langle\langle cz \rangle\rangle = 2630$; $cz_{max} = 8053$)

STATISTIC	OBSERVED VALUE	PREDICTED VALUES C1	PREDICTED VALUES C2	ERRORS C1	ERRORS C2
s_m	0.64	0.78 ± 0.03	0.62 ± 0.03	4.0	0.8
β	1.93	2.66 ± 0.24	1.74 ± 0.24	3.0	0.8
ϱ_1	−0.66	-0.50 ± 0.04	-0.69 ± 0.03	3.7	0.9
σ_1	0.75	0.75 ± 0.03	0.76 ± 0.04	0.1	0.3
ϱ_2	−0.16	0.04 ± 0.06	-0.22 ± 0.07	4.1	0.8
σ_2	0.57	0.65 ± 0.03	0.56 ± 0.03	2.7	1.9

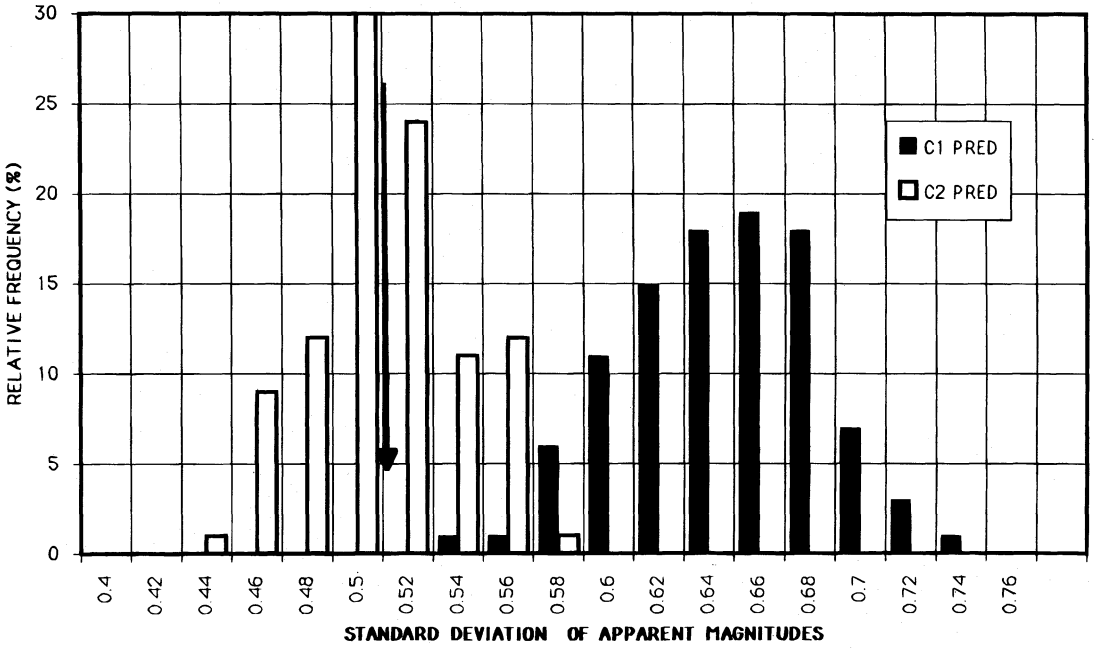

FIG. 7.—Same as Fig. 3 for sample G

© American Astronomical Society • Provided by the NASA Astrophysics Data System

1996ApJ...465..578S

TABLE 11

STATISTICAL ANALYSIS OF THE SUBSAMPLE WITH $cz > 2000$, $m \leq 12$ ($N = 130$; $\langle cz \rangle = 3286$; $\langle\langle cz \rangle\rangle = 3125$; $cz_{max} = 8053$)

Statistic	Observed Values	Predicted Values C1	Predicted Values C2	Errors C1	Errors C2
s_m	0.52	0.65 ± 0.04	0.52 ± 0.03	3.8	0.2
β	1.79	2.66 ± 0.30	1.81 ± 0.26	2.9	0.1
ϱ_1	−0.68	-0.50 ± 0.05	0.68 ± 0.04	3.5	0.2
σ_1	0.63	0.63 ± 0.03	0.63 ± 0.03	0.1	0.1
ϱ_2	−0.20	0.04 ± 0.07	0.19 ± 0.07	3.3	0.1
σ_2	0.47	0.55 ± 0.03	0.47 ± 0.03	2.8	0.2

be excessive at larger redshifts but will have much reduced impact there. The effect of a fixed increase in the observed redshifts by 300 km s^{-1} would appear likely to majorize, or at the very least represent the order of magnitude of the effect. But this hypothetical perturbation has no effect on the comparative fits of C1 and C2 and little effect on the overall fit of the C1 predictions.

Tables 13 and 14 summarize the results of analysis on the same basis as in Tables 2–5, when 300 km s^{-1} is added to the redshifts of samples A and G. There appears to be a modest improvement for *both* C1 and C2 in the extremely low redshift region, consistent with the existence of a highly localized effect. But in the higher redshift sample there is no appreciable effect. In any event, since the mathematical effect of the perturbation is to decrease the effective slope of the theoretical C1 magnitude-redshift relation, thus displacing it in the direction of the C2 relation, some improvement in the quality of the fit of the C1 predictions was to be expected.

TABLE 12

STATISTICAL ANALYSIS OF THE SUBSAMPLE WITH $cz > 2500$, $m \leq 12.4$ ($N = 97$; $\langle cz \rangle = 3652$; $\langle\langle cz \rangle\rangle = 3517$; $cz_{max} = 8053$)

Statistic	Observed Value	Predicted Values C1	Predicted Values C2	Errors C1	Errors C2
s_m	0.45	0.58 ± 0.04	0.47 ± 0.04	3.8	0.6
β	1.49	2.55 ± 0.36	1.67 ± 0.36	2.9	0.5
ϱ_1	−0.70	-0.49 ± 0.06	-0.67 ± 0.05	3.4	0.6
σ_1	0.58	0.58 ± 0.04	0.57 ± 0.04	0.0	0.2
ϱ_2	−0.27	0.01 ± 0.08	-0.22 ± 0.09	3.4	0.6
σ_2	0.43	0.50 ± 0.03	0.44 ± 0.03	0.6	0.3

TABLE 13

STATISTICAL ANALYSIS OF THE SUBSAMPLE WITH $cz > 500$, $m \leq 12.4$, WHEN 300 km s^{-1} IS ADDED TO THE OBSERVED REDSHIFTS

Statistic	Observed Value	Predicted Values C1	Predicted Values C2	Errors C1	Errors C2
s_m	0.75	0.95 ± 0.04	0.73 ± 0.03	5.8	0.5
β	2.07	2.92 ± 0.18	2.01 ± 0.17	4.8	0.3
ϱ_1	−0.70	-0.50 ± 0.04	0.71 ± 0.02	5.2	0.5
σ_1	0.86	0.86 ± 0.02	0.86 ± 0.03	0.0	0.1
ϱ_1	−0.14	0.11 ± 0.05	-0.16 ± 0.06	5.5	0.4
σ_2	0.62	0.75 ± 0.03	0.61 ± 0.03	4.6	0.2

8. THE MEAN APPARENT MAGNITUDE AS A FUNCTION OF REDSHIFT

The several statistics studied above do not, of course, exhaust the possibilities. A directly observable relation that was not treated above is that between the observed and predicted mean magnitude-redshift relation in redshift bins. However, unlike those above, this does not provide a unique individual statistic whose significance level is well

TABLE 14

STATISTICAL ANALYSIS OF THE SUBSAMPLE WITH $cz > 2000$, $m \leq 12.4$, WHEN 300 km s^{-1} IS ADDED TO THE OBSERVED REDSHIFTS

Statistic	Observed Value	Predicted Values C1	Predicted Values C2	Errors C1	Errors C2
s_m	0.52	0.63 ± 0.03	0.51 ± 0.03	3.4	0.4
β	1.94	2.82 ± 0.30	1.83 ± 0.28	2.9	0.4
ϱ_1	−0.63	-0.45 ± 0.05	-0.65 ± 0.04	3.3	0.4
σ_1	0.59	0.59 ± 0.03	0.60 ± 0.03	0.0	0.2
ϱ_2	−0.15	0.07 ± 0.07	-0.18 ± 0.07	3.2	0.0
σ_2	0.46	0.53 ± 0.03	0.46 ± 0.03	2.1	0.1

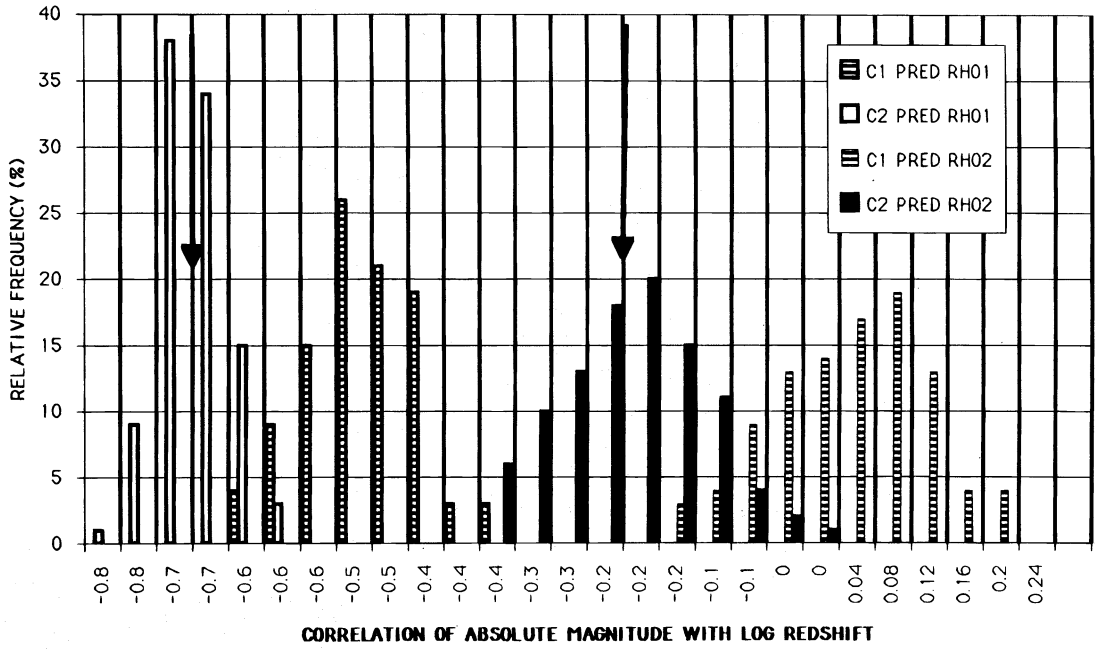

FIG. 8.—Same as Figure 4 for sample G

© American Astronomical Society • Provided by the NASA Astrophysics Data System

1996ApJ...465..578S

defined. In addition, it appears cosmologically much less sensitive than s_m and ϱ_p, and it has already been treated in several respects. In Segal (1986a), the observed mean magnitude to redshift relation was compared with the predictions of a variety of redshift-distance power laws, using 10 equal-sized redshift bins. On average, the C1 deviations were twice those of the C2 deviations and 50% larger than those of the cubic law C3. In addition, the slope of the predicted C1 relation was consipicuously steeper than that of the observed relation, as shown in Segal (1989).

The large deviation of the C1 prediction in the lowest redshift bin cannot be ascribed to a local perturbation, since it is qualitatively entirely similar to the corresponding deviation for the subsample at redshifts in excess of 2000 km s^{-1} and is shown in other samples, e.g., Segal (1989), and at higher redshifts, Segal et al. (1994a). The statistics of the $\langle m \mid z \rangle$ relation for sample A are summarized in Table 15. A less detailed summary of the statistics for all the samples, both in their original form and after the addition of 300 km s^{-1} to the observed redshifts, is given in Table 16 (see below).

These tables were computed by placing the redshifts in increasing order and dividing the sample into 10 equal-sized bins (deleting a possible smaller number of galaxies remaining at the highest redshifts). The observed mean apparent magnitude is then computed for each bin, together with its standard deviation, and compared with the value predicted by each cosmology from its RLF. This procedure is identical to that used in earlier studies; see Segal et al. (1993) for the analytic expression of the predicted mean giving statistically consistent correction for the observational magnitude cutoff (or "Malmquist" bias). The results for sample A are summarized in Figure 9. Whether in terms of the mean

TABLE 15

OBSERVED AND PREDICTED VALUES OF $\langle m \mid z \rangle$ FOR SAMPLE A

$\langle\langle z \rangle\rangle$	OBSERVED $\langle m \rangle$	DISPERSION IN $\langle m \rangle$	PREDICTIONS OF $\langle m \rangle$	
			C1	C2
763.....	10.38	0.12	9.65	10.24
1037.....	10.81	0.12	10.30	10.57
1243.....	10.74	0.16	10.63	10.75
1466.....	10.85	0.10	10.93	10.91
1744.....	10.98	0.16	11.08	11.09
2004.....	11.24	0.11	11.19	11.23
2386.....	11.32	0.09	11.38	11.36
2853.....	11.46	0.10	11.56	11.47
3471.....	11.62	0.07	11.71	11.59
4908.....	11.84	0.06	11.93	11.78

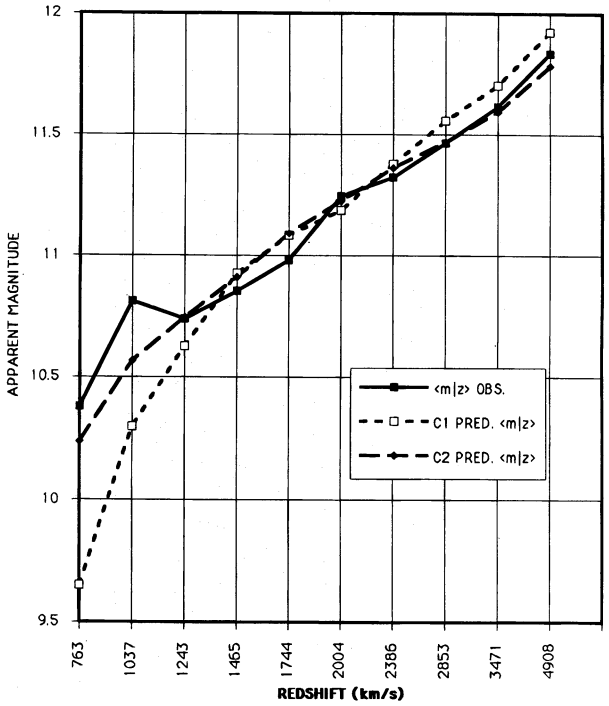

FIG. 9.—Observed and predicted $\langle m \mid z \rangle$ relations for sample A

magnitude for the whole sample in question, or the rms error for the mean magnitudes of the 10 bins, or the overall slope of the predicted $\langle m \mid z \rangle$ relation, the C1 deviations are several times those of C2. The C1 deviation in its $\langle m \mid z \rangle$ prediction is largest in the first bin and exceeds the standard deviation of the observed magnitudes in this bin by 6 σ; the corresponding C2 deviation is only 0.1 σ.

The C1 $\langle m \mid z \rangle$ prediction deviations for sample A decrease as the redshift increases, which again might suggest that they arise from a nongeneric effect, such as a local perturbation, at the lowest redshifts. This possibility is addressed by the analysis of all the samples shown in Table 16. In addition to the $\langle m \mid z \rangle$ predictions in each of the 10 bins, $\langle m \rangle$ was predicted for the entire sample, and in addition in each of two equal-sized bins into which the sample was divided (with the possible deletion of the highest redshift observation). The overall mean deviations, i.e., those for the entire sample, are denoted as $\delta\langle m \rangle$, taken as positive for predictions that are too bright. The rms of the respective 10 prediction errors are denoted as RMSp. The slope errors, or errors in $\partial\langle m \mid z \rangle / \partial \log cz$, are denoted as $\delta\lambda$ and are two-point estimates between the means of the two equal-

TABLE 16

STATISTICS OF THE $\langle m \mid z \rangle$ RELATION IN DIVERSE SAMPLES

Sample	$\langle\langle cz \rangle\rangle$	$\langle m \rangle_{obs}$	$\delta\langle m \rangle_{C1}$	$\delta\langle m \rangle_{C2}$	RMS_{C1}	RMS_{C2}	$\delta\lambda_{C1}$	$\delta\lambda_{C2}$
A	1891	11.13	0.09	0.03	0.29	0.10	0.74	0.08
B	1779	10.99	0.12	0.04	0.24	0.12	0.43	−0.09
C	1616	10.79	0.12	0.05	0.23	0.15	0.62	0.09
D	1325	10.66	0.07	0.03	0.21	0.14	0.87	0.34
E	2171	11.22	0.07	0.02	0.23	0.09	0.90	0.00
F	2630	11.37	0.06	0.02	0.18	0.12	0.99	−0.12
G	3125	11.51	0.05	0.01	0.15	0.07	0.97	−0.05
H	3517	11.61	0.03	0.01	0.17	0.10	1.33	0.31
A*	2231	11.13	0.06	0.02	0.17	0.08	0.77	−0.13
E*	2499	11.22	0.06	0.02	0.19	0.09	0.86	−0.16
F*	2948	11.37	0.06	0.02	0.16	0.13	0.92	−0.24
G*	3438	11.51	0.04	0.01	0.14	0.08	0.95	−0.22

© American Astronomical Society • Provided by the NASA Astrophysics Data System

1996ApJ...465..578S

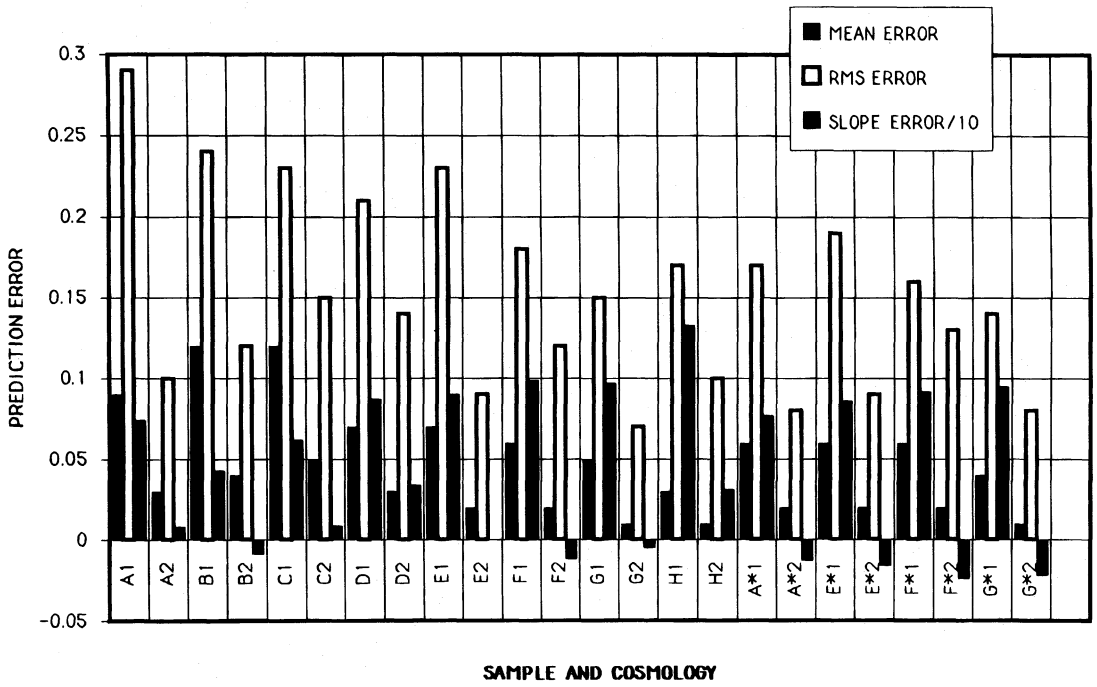

FIG. 10.—Errors of the $\langle m \mid z \rangle$ predictions in diverse samples

sized bins; e.g., in sample A there are two bins of 145 galaxies each, having mean redshifts 1203 and 2973 (where our usage is that "mean" redshift means geometric mean $\langle\langle z \rangle\rangle$ unless otherwise stated). The mean prediction errors for the first and second bins are 0.236 and −0.054, indicating a slope error of $[0.026 - (-0.054)]/(\log 2973 - \log 1203)$.

Table 16 is summarized by Figure 10. These results indicate that a systematic irregularity at lower redshifts, such as a gravitational effect arising from the overdensity of the Milky Way, is not responsible for the apparently significant deviations of the C1 $\langle m \mid z \rangle$ predictions from observation. The excessive brightness of the C1 predictions for $\langle m \mid z \rangle$ at the lower redshifts of a given sample appears to be a quite general feature, irrespective of the average redshift of the sample. Figure 11 shows this for sample G ($cz > 2000$).

To be sure, some of the C1 predictions are not significantly deviant, as noted already for the standard deviation of the residuals, and perhaps for the mean apparent magnitude of the entire sample. But even the C3 predictions for these quantities are no less accurate, and occasional consistency can, according to elementary principles of scientific methodology, hardly exculpate large model-independent inconsistencies.

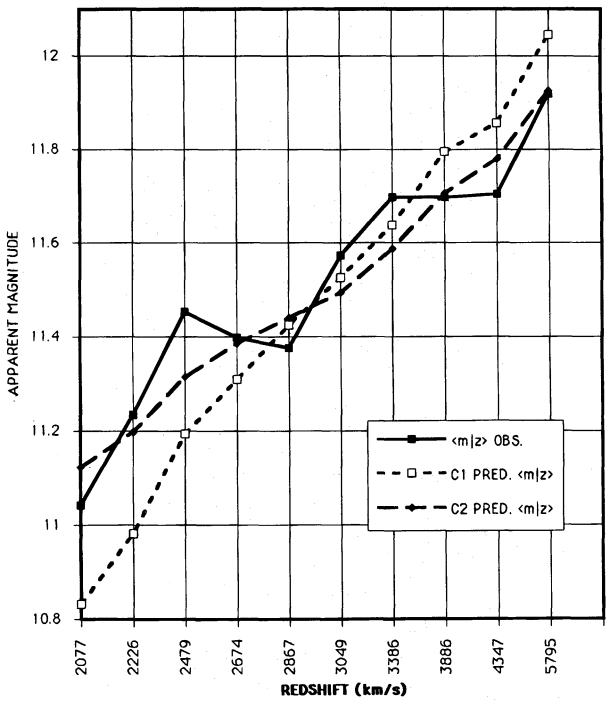

FIG. 11.—Same as Fig. 9 for sample G

9. THE MAGNITUDE- AND REDSHIFT-LIMITED HALF-SAMPLES

Because of the traditional and present widespread acceptance of the linear law, we treat two further samples, which might be expected to show the linear law at its best: (i) the brightest half-sample; (ii) the lowest redshift half-sample. The brightest half-sample in the range $cz > 500$ km s^{-1} is that for which $m \leq 11.24$, and it consists of 145 galaxies. Table 17 shows the main predictions of the linear and square laws on the same basis as earlier. There is no indication whatsoever for the improvement in the accuracy of the C1 predictions that would be expected if incompleteness

TABLE 17

STATISTICAL ANALYSIS OF THE SUBSAMPLE WITH $m \leq 11.24$, $cz > 500$ (145 GALAXIES; $\langle cz \rangle = 1584$; $cz_{max} = 4744$)

STATISTIC	OBSERVED VALUES	PREDICTED VALUES		ERRORS (σ)	
		C1	C2	C1	C2
s_m	0.55	0.72 ± 0.05	0.58 ± 0.04	3.1	0.6
β	1.01	1.52 ± 0.31	1.16 ± 0.23	1.7	0.7
ϱ_1^B	−0.84	-0.72 ± 0.04	-0.82 ± 0.03	2.6	0.7
ϱ_1^A	−0.05	-0.03 ± 0.06	-0.12 ± 0.05	0.3	1.0
ϱ_2^B	−0.50	-0.28 ± 0.09	-0.44 ± 0.07	2.4	0.7
ϱ_2^A	0.00	0.15 ± 0.07	-0.02 ± 0.07	2.1	0.3

© American Astronomical Society • Provided by the NASA Astrophysics Data System

1996ApJ...465..578S

TABLE 18

STATISTICAL ANALYSIS OF THE SUBSAMPLE WITH $500 < cz \leq 1879$, $m < 12.4$ (145 GALAXIES; $\langle cz \rangle = 1258$; $cz_{max} = 1879$)

STATISTIC	OBSERVED VALUE	PREDICTED VALUES		ERRORS (σ)	
		C1	C2	C1	C2
s_m	0.75	0.99 ± 0.05	0.79 ± 0.05	4.9	1.0
β	1.46	4.00 ± 0.54	2.35 ± 0.38	4.7	2.3

were a factor. The lowest redshift half-sample in the range $cz > 500$ km s^{-1} consists of the 145 galaxies for which $cz < 1879$. The cosmology-independent predictions on the same basis as earlier are shown in Table 18. Again, there is no relative improvement in the accuracy of the predictions for C1. Moreover, the RLF1 for this subsample is considerably fainter than that for sample A, indicating the same apparent luminosity evolution as discussed above. The effect of local irregularities such as Virgo might be considered to weaken this conclusion, but the RLF2 for the subsample is quite consistent with that for sample A, and the C2 predictions remain accurate.

10. SPECTRAL INDEX AND EXACT COSMOLOGY EFFECTS

Although no significant effects of these types are expected at the very low redshifts involved here, it is reassuring to make quantitative estimates of them. Observed spectral indices are lacking, but an order-of-magnitude upper bound on the effect of their possible deviations from unity may be obtained by taking a wide range around the spectral index $\alpha = 1$ implicitly involved in the above analysis and computing the effects on the basic statistics for the extreme values. For the assumed values $\alpha = 0$ and 2, the results for ϱ_1 and σ_1 are within the ranges from -0.780 to -0.784 and 0.980 to 0.987, respectively, with the value for $\alpha = 1$ approximately the mean of the extreme values. The corresponding ranges for ϱ_2 and σ_2 are -0.259 to -0.272 and 0.635 to 0.637. These variations are clearly inconsequential, and taking into account that these approximate the extreme ranges, whereas an effective sample average spectral index may be expected to be less extreme, the actual effect is probably even less.

The C1 magnitude-redshift law is identical to that for FLC with $q_0 = 1$ and $\Lambda = 0$. For the assumed value $q_0 = 0$, ϱ_1 is increased by 0.002, while σ_1 is reduced by 0.003. The CC law gives the respective values -0.265 and 0.636 for ϱ_2 and σ_2, or differences of 0.007 and 0.001 from the corresponding C2 statistics, which are again inconsequential.

11. DISCUSSION

The phenomenological inconsistency of the linear law that has been documented above leaves evolution in the very low redshift regime as the only apparent way to save the linear law. On the other hand, if the linear law does not apply in its original nonevolutionary form to direct observations in any regime, its standing as a scientific, and in particular falsifiable, hypothesis is seriously impugned. The intuitive simplicity of a Doppler theory of the redshift may commend it to consideration, but if in many decades no clearly equitable and objective direct observational validation for it has been attained (in fact, it is strongly contraindicated), it remains a preliminary hypothesis, as described by Hubble & Tolman. In any event, a Doppler theory is not necessarily implicative of the Hubble law, e.g., a square or even a cubic law is consistent with sufficiently special forms of FLC.

The apparent clear-cut evolution within the frame of C1 that is indicated by the present analysis can hardly be avoided by limitations to even lower redshifts. Not only do local irregularities and peculiar motions become highly significant at materially lower redshifts than those of the last sample considered, but possible sample sizes decrease rapidly at the same time, indicating probable statistical mootness. The fact that this apparent evolution is closely similar to that found in higher redshift samples, e.g., the quasar sample of Schmidt & Green (1983) or the active galactic nucleus sample of Stocke et al. (1991), within the frame of Friedmann cosmology with parameters in the range normally considered realistic, suggests that the Doppler theory of the redshift is unsound in some fundamental fashion.

In contrast, C2 is consistent with the present observations, and many other complete samples at small, intermediate, and large redshifts (e.g., Segal et al. 1993; Segal 1980, 1986a, b, 1989, 1993; Segal & Nicoll 1986, 1992, 1996; Nicoll & Segal 1978, 1982; Nicoll et al. 1980). In addition, it explains fully the deviations of the predictions made by the Friedmann model; and its freedom from cosmological parameters such as q_0 and Λ, as well as from evolution, render it in principle as well as in practice more efficient as a model applicable to direct observations, rather than merely to internal theoretical or model-dependent quantities. There is no apparent scientific reason not to use it for this purpose.

We thank a referee for useful suggestions.

APPENDIX

A referee has noted a discrepancy between the ROBUST LF and his own estimate of the LF based on four clusters represented in V79, which represent approximately one-fourth the sample. Since it is a priori conceivable that the cluster-based LF could restore the Hubble law to consistency with V79, and also because the referee's method of LF estimation is in common usage, it appears desirable to examine quantitatively the implications of the alternative LF.

As noted above, the use of cluster-based estimates of the LF, although traditional, is inherently model dependent, since peculiar velocities cannot be separated observationally from the total observed redshift, and since only the two-dimensional projection of the spatial distribution of the cluster galaxies is observed, rendering assignments of cluster membership uncertain. However, any given LF is testable on the same basis as above, by comparison of its hard predictions with direct observation. The referee's estimate is shown in Figure 12.

Directly observable predictions from the referee's cluster-based LF have been determined, using the quite conservative limiting magnitude 11.5 mag that he proposed. They are, however, considerably *more*, rather than *less*, deviant than the C1

© American Astronomical Society • Provided by the NASA Astrophysics Data System

1996ApJ...465..578S

predictions derived from RLF1, which are already significantly deviant. This contrasts with the C2 predictions derived from RLF2, which as shown above are extremely accurate.

To clarify the background, the referee's report is quoted, as follows:

> Since I was asked to referee this article, I decided I would look a little harder at some aspect of the analysis. If I could see some major flaw in one area of the argument I could stop there. So I looked at the issue of the luminosity functions....
>
> The authors use a program that they call ROBUST to develop these luminosity functions.... However, there is an easy way to have a rough evaluation of whether it is getting reasonable results. Approximately a quarter of the galaxies in various samples that they use in the paper are drawn from only four clusters; half of these are in the Virgo Cluster alone (in my analysis here I follow the authors and strictly accept the data given in a paper by Visvanathan). The four clusters have close to the same redshifts so the differences between cosmological models are small with this substantial fraction of the entire sample.
>
> The relative luminosity function within a specific cluster above the magnitude completeness limit can be determined simply, since all the galaxies are at the same distance. I used the Segal-Nicoll recipe to convert to absolute magnitudes using the mean cluster redshift with the convention $m = M$ at 2000 km/s. Doradus has a smaller redshift than Virgo so I just consider the completeness in that case to the shallower Virgo limit. Fornax and Eridanus have essentially identical and slightly larger redshifts so are complete to a less deep limit than Virgo. The four cluster data can be superimposed to create luminosity functions with only minor adjustments for the slightly different incompletion cutoffs....

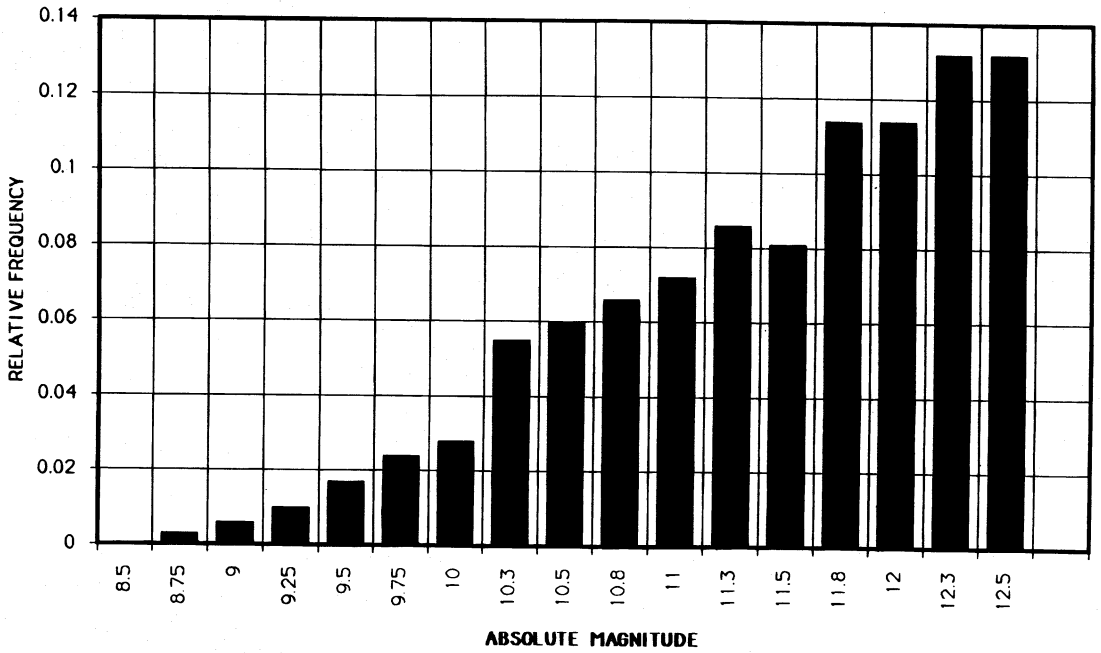

FIG. 12.—Cluster-based estimate of the C1 differential luminosity function for the subsample of Fig. 13

TABLE 19

STATISTICAL ANALYSIS OF THE SUBSAMPLE WITH $m \leq 11.5$, $cz > 500$
(188 GALAXIES; $\langle cz \rangle = 1756$; $cz_{max} = 4910$)

STATISTIC	OBSERVED VALUE	PREDICTIONS			ERRORS (σ)		
		C1*	C1	C2	C1*	C1	C2
s_m	0.60	0.87 ± 0.05	0.76 ± 0.05	0.60 ± 0.03	5.4	3.0	0.0
β	1.23	2.27 ± 0.25	1.75 ± 0.25	1.23 ± 0.21	4.7	2.1	0.0
ϱ_1	−0.82	-0.62 ± 0.05	-0.72 ± 0.04	-0.82 ± 0.02	4.6	2.6	0.0
σ_1	0.96	0.93 ± 0.03	0.95 ± 0.03	0.96 ± 0.04	1.1	0.3	0.0
ϱ_2	−0.44	-0.07 ± 0.07	-0.23 ± 0.08	-0.44 ± 0.06	5.7	2.6	0.0
σ_2	0.6	0.76 ± 0.04	0.68 ± 0.03	0.61 ± 0.04	3.8	2.3	0.0
ϱ_1^A	−0.07	-0.01 ± 0.05	-0.02 ± 0.05	-0.13 ± 0.04	1.1	1.0	1.5
σ_1^A	0.93	0.90 ± 0.04	0.97 ± 0.04	0.93 ± 0.05	1.8	1.0	0.0
ρ_2^A	0.04	0.25 ± 0.06	0.19 ± 0.06	-0.03 ± 0.06	3.4	2.4	1.3
σ_2^A	0.67	0.76 ± 0.04	0.73 ± 0.04	0.66 ± 0.03	2.3	1.9	0.1

NOTE.—C1* = C1 with RLF1 replaced by the (cited) cluster-based LF.

© American Astronomical Society • Provided by the NASA Astrophysics Data System

1996ApJ...465..578S

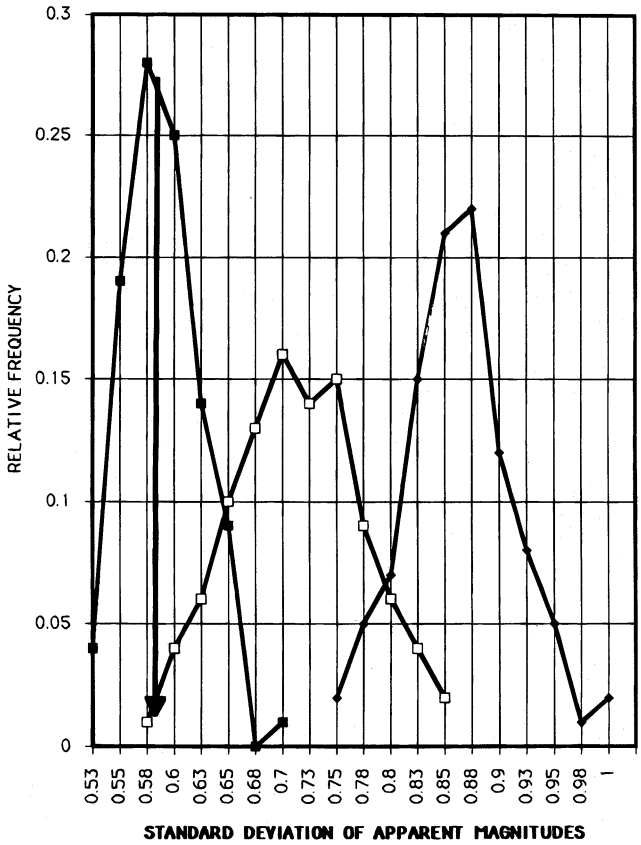

FIG. 13.—Predicted distributions of the dispersion in apparent magnitude for the subsample $m \leq 11.5$, $cz > 500$ (188 galaxies). *Filled squares*, C2; *open squares*, C1 (using RLF1); *filled diamonds*, C1 using cluster-based estimate of luminosity function. Arrow shows the observed value.

> It can be seen that the luminosity functions built from ~1/4 of the data hardly resembles the luminosity functions of the whole sample built with ROBUST. In the first place, it is evident that the Visvanathan sample is *not* complete to 12.4 mag. Incompletion sets in at 11.5 mag.... The very different luminosity functions I get with simple assumptions and a significant fraction of the data look like the conventional Schechter-type functions where incompletion is kicking in near M^*. The ROBUST procedure is not very robust.

Notwithstanding the model dependence of the claim that incompleteness sets in at 11.5 mag (V79 [p. 85] states, "From Fig. 1 it can be seen that the limiting magnitude of the catalog is 12.4 in $V_m^{K,E}$"), we have tested the cluster-based LF estimated on the subsample defined by the 11.5 mag limit, inclusive of 188 galaxies. The same statistics as earlier were predicted using 100 random samples drawn from the cluster-based LF estimate, and also from RLF1 and RLF2 for this subsample. The results are summarized in Table 19. The major C1 predictions based on the ROBUST LF are far less deviant than those derived from the cluster-based LF.

The results are shown in greater detail for the especially informative statistic s_m in Figure 13. This indicates that the predictions of the cluster-based LF appear remote from any likelihood of attaining the observed value, irrespective of the number of random samples that might be constructed.

REFERENCES

de Vaucouleurs, G. 1972, in IAU Symp. 44, External Galaxies and Quasi-Stellar Objects, ed. D. S. Evans, D. Wills, & B. J. Wills (Dordrecht: Reidel), 753
Hawkins, G. S. 1964, Nature, 194, 563
Hubble, E., & Tolman, R. C. 1935, ApJ, 82, 302
McVittie, G. C. 1965, General Relativity and Cosmology (Champaign: Univ. Illinois Press)
Nicoll, J. F., Johnson, D., Segal, I. E., & Segal, W. 1980, Proc. Natl. Acad. Sci., 77, 6275
Nicoll, J. F., & Segal, I. E. 1978, Ann. Phys., 113, 1
———. 1980, A&A, 82, L3
———. 1982, A&A, 115, 398
———. 1983, A&A, 118, 180
Saunders, W., Rowan-Robinson, M., Lawrence, A., Efstathiou, G., Kaiser, N., Ellis, R. S., & Frenk, C. S. 1990, MNRAS, 242, 318
Schmidt, M., & Green, R. F. 1983, ApJ, 269, 352
Segal, I. E. 1976, Mathematical Cosmology and Extragalactic Astronomy (New York: Academic)
———. 1980, MNRAS, 192, 755
Segal, I. E. 1986a, Proc. Natl. Acad. Sci., 83, 7129
Segal, I. E. 1986b, PASJ, 38, 611
———. 1989, MNRAS, 237, 17
———. 1993, Proc. Natl. Acad. Sci., 90, 4798
Segal, I. E., & Nicoll, J. F. 1986, ApJ, 300, 224
———. 1992, Proc. Natl. Acad. Sci., 89, 11669
———. 1996, ApJ, 459, 496
Segal, I. E., Nicoll, J. F., & Blackman, E. 1994a, ApJ, 430, 63
Segal, I. E., Nicoll, J. F., & Wu, P. 1994b, ApJ, 431, 52
Segal, I. E., Nicoll, J. F., Wu, P., & Zhou, Z. 1991, Naturwissenschaften, 78, 289
———. 1993, ApJ, 411, 465
Segal, I. E., & Zhou, Z. 1995, ApJS, 100, 307
Shapley, H., & Ames, A. 1932, Harvard Ann., 88, 2
Stocke, J. T., Morris, S. L., Gioia, I. M., Maccacaro, T., Schild, R., Wolter, A., & Henry, J. P. 1991, ApJS, 76, 813
Strauss, M. A., Davis, M., Yahil, A., & Huchra, J. P. 1990, ApJ, 361, 49
Visvanathan, N. 1979, ApJ, 228, 81 (V79)
Wilks, S. S. 1962, Mathematical Statistics (New York: Wiley)
Yahil, A., Strauss, M., Davis, M., & Huchra, J. P. 1991, ApJ, 372, 380

© American Astronomical Society • Provided by the NASA Astrophysics Data System